A Nature Portfolio journal



https://doi.org/10.1038/s42003-025-08893-0

Common DNA sequence variation influences epigenetic aging in African populations

Check for updates

Gillian L. Meeks ¹, Brooke Scelza², Hana M. Asnake³, Sean Prall ², Etienne Patin ⁴, Alain Froment⁵, Maud Fagny ^{4,6}, Lluis Quintana-Murci^{4,7}, Brenna M. Henn ^{8,9} & Shyamalika Gopalan ^{10,11,12} ⊠

Aging is associated with genome-wide changes in DNA methylation in humans, facilitating the development of epigenetic age prediction models. However, these models have been trained primarily on European-ancestry individuals and none account for the impact of methylation quantitative trait loci (meQTL). To address these gaps, we analyze the relationships between age, genotype, and CpG methylation in 3 understudied populations: central African Baka (n = 35), southern African ‡Khomani San (n = 52), and southern African Himba (n = 51). We show that published prediction methods yield higher mean errors in these cohorts compared to European-ancestry individuals and find that unaccounted-for DNA sequence variation may be a significant factor underlying this loss of accuracy. We leverage information about the associations between DNA genotype and CpG methylation to develop an age predictor that is minimally influenced by meQTL and show that this model remains accurate across a broad range of genetic backgrounds. Intriguingly, we also find that the older individuals and those with lower epigenetic age acceleration carry more genetic variants linked to reduced epigenetic age. These findings support the hypothesis that multiple heritable factors collectively influence healthspan and longevity in human populations.

The aging process is associated with significant, genome-wide epigenetic changes. In particular, DNA methylation levels at specific cytosine-guanine dinucleotides (CpGs) are strongly associated with chronological age, driving the development of a suite of age prediction algorithms referred to as 'epigenetic clocks'. While thousands of CpG sites across the genome exhibit consistent patterns of increasing or decreasing DNA methylation with age¹⁻³, accurate age predictors can be constructed from remarkably few CpGs⁴⁻¹¹. The first DNA methylation-based predictors were trained on individuals' chronological age (i.e., the actual number of years lived), and found that epigenetic clocks could be more accurate and precise than other molecular methods of age estimation, such as telomere length¹²⁻¹⁴. Subsequent research found that the error in epigenetic clock-based age estimates (i.e., the deviation between true and predicted age) is also biologically

meaningful, and that accelerated epigenetic age is associated with multiple age-related diseases¹⁵⁻¹⁸. This observation spurred the next generation of epigenetic predictors, which included PhenoAge¹⁹, GrimAge^{20,21}, and FitAge²², that were specifically trained to predict morbidity, mortality, and other aspects of biological aging.

Deviation between one's predicted and actual age, i.e., epigenetic age acceleration, is influenced by a host of environmental and lifestyle factors²³, leading researchers to examine its relationship to systemic health disparities experienced by minorities in cosmopolitan populations^{24–31}. However, these epigenetic clocks are almost exclusively trained on European-descent populations living in industrialized societies and are rarely validated across a range of genetic backgrounds and environmental contexts. Studies that have assessed popular predictors in genetically diverse cohorts find inconsistent

¹Integrative Genetics and Genomics Graduate Program, University of California Davis, Davis, CA, USA. ²Department of Anthropology, University of California Los Angeles, Los Angeles, CA, USA. ³Forensic Science Graduate Program, University of California Davis, Davis, CA, USA. ⁴Human Evolutionary Genetics Unit, CNRS UMR2000, Paris, France. ⁵Institut de Recherche pour le Développement, UMR 208, Muséum National d'Histoire Naturelle, Paris, France. ⁶Université Paris-Saclay, INRAE, CNRS, AgroParisTech, Genetique Quantitative et Evolution - Le Moulon, Gif-sur-Yvette, France. ⁷Chair Human Genomics and Evolution, Collège de France, Paris, France. ⁸Department of Anthropology, University of California Davis, Davis, CA, USA. ⁹UC Davis Genome Center and Center for Population Biology, University of California Davis, Davis, CA, USA. ¹⁰Department of Genetics and Biochemistry, Clemson University, Clemson, SC, USA. ¹²Center for Human Genetics, Clemson University, Greenwood, SC, USA. ¹²Center for Human Genetics, Clemson University, Greenwood, SC, USA. ¹²Center for Human Genetics, Clemson University, Greenwood, SC, USA.

Communications Biology | (2025)8:1530

patterns. For example, both African-American and Hispanic cohorts exhibit systematically higher epigenetic age under some clocks but systematically lower epigenetic age under others^{19,32–34}. Similarly, a recent study found previously identified signals of epigenetic age acceleration in European-ancestry Alzheimer's disease patients³⁵ did not replicate in admixed, diverse ancestry cohorts³⁶. Finally, while many of these clocks have been applied to diverse African populations from places such as South Africa³⁷, Ghana³⁸, and Côte d'Ivoire³⁹, some exhibit lower predictive accuracy compared to European cohorts, indicating reduced transferability in these contexts. Systematic differences among or within populations might reflect real variation in the aging process, but without first confirming that epigenetic clocks maintain their predictive power across diverse population contexts, researchers should be cautious about interpreting the causes and consequences of epigenetic age acceleration in relation to human health⁴⁰.

A few recent studies have found that prediction accuracy does indeed decline when clocks trained on one genetic ancestry are applied to individuals of a diverged genetic ancestry^{36,41–43}, mirroring findings from studies of polygenic risk score (PRS) transferability^{9,41–45}. This observation might be partially explained by the relatively high heritability of DNA methylation and the strong influence of individual single nucleotide polymorphisms (SNPs)^{46–48}; 10% of CpG sites exhibit heritability greater than 50%, and up to 45% of CpG sites assayed by the Illumina 450k array show influence of methylation quantitative trait loci (meQTL), 90% of which act locally, in *cis*⁴⁹. This significant genetic control of DNA methylation also explains why genome-wide variation in DNA methylation broadly recapitulates patterns of population structure observed in human genetic data^{50–55}.

Previous work has identified meQTL as being important drivers of variation at some age-associated CpGs^{12,13,36,56}. If CpGs influenced by meQTL are used to construct an epigenetic clock, its accuracy might be expected to decline when applied to a genetically diverged population, as predictor coefficients will be biased by the meQTL frequency of the training cohort.

In order to address these issues, we test several popular epigenetic clocks on genetically diverse populations and characterize the influence of genetic variation on DNA methylation both within and across populations. We analyze saliva-derived DNA methylation data from three African populations representing a broad swath of genetic ancestry: Baka central African foragers, southern African ‡Khomani San foragers, and southern African Himba pastoralists. Each of these groups has a distinct, complex evolutionary history and currently occupies different ecological regions across the continent, generating among-population variation in both genetic and environmental factors that can influence DNA methylation. We compare the predictive accuracy of 10 published epigenetic clocks on these African cohorts to publicly available data more closely matching the vast majority of predictor training data, from European-ancestry and Hispanic/ Latino cohorts³⁴. Using paired genotype data for the African individuals in our dataset and newly available, ancestry-matched imputation panels⁵⁷, we estimate heritability and identify significant cis-meQTL for age-associated CpGs across the genome. Importantly, we find that a large proportion of CpGs included in established predictors are influenced by meQTL identified in our modestly-sized cohorts. We show that not accounting for genetic variation at meQTL contributes to error in epigenetic age prediction and develop epigenetic clocks that specifically exclude CpGs with significant cisheritability. Finally, we develop a genotype-based 'epigenetic aging score' (EAS), which captures the effects of epigenetic age-increasing variants from across the genome under an additive model. We find that EAS correlates with independently derived estimates of epigenetic age acceleration, suggesting biologically meaningful effects at some of these meQTL (Study design in Supplementary Fig. 1).

Results

Evaluating the performance of published age predictors on African cohorts

We tested 10 age prediction methods (see "Methods" section) that were trained primarily on European-ancestry cohorts living in Europe and the United States: the Horvath multi-tissue age predictor¹², the Hannum blood clock¹³, the Horvath skin and blood clock⁵⁸, the Zhang elastic net predictor⁵⁹, PhenoAge¹⁹, two iterations of GrimAge, both using either true or predicted age^{20,21}, and FitAge²². We applied the predictors to saliva-derived DNA methylation data from 3 African cohorts and compared performance to a publicly available tissue-matched dataset of European-ancestry and Hispanic/Latino individuals (GEO accession GSE7887434). Because some clocks show age-dependent accuracy60, we focus on age-adjusted prediction errors when comparing populations to account for the different age distributions across cohorts. We found that 9 of the predictors exhibited significant differences in age-adjusted error between at least one African population and the European and Hispanic/Latino datasets (Fig. 1; Supplementary Tables 1 and 2; Supplementary Figs. 2 and 3). There was not a consistent pattern of over- or under-estimation for the African cohorts relative to the European and Hispanic/Latino individuals; for example, the Himba as a group were estimated to be younger than Europeans by most clocks, but older by GrimAge2 based on true age; ‡Khomani San individuals were estimated to be younger than Europeans and Hispanic/Latino individuals by the Hannum and Zhang clocks, but older by FitAge and GrimAge. We also found significant differences in prediction error among the three African cohorts. Only the Horvath multi-tissue clock showed no differences in age-adjusted error in the African samples as compared to the European and Hispanic/Latino samples.

We considered that differences in predictive accuracy might be due to variation in cell-type composition. Although all the samples were nominally saliva-derived and we restricted comparisons to samples predicted to be saliva or blood-derived (see "Methods" section), significant among-population variation in the proportions of white blood cell types and epithelial cells might still exist. With the exception of the Horvath multi-tissue clock¹² and the skin and blood clock⁵⁸, the predictors that we evaluated were trained primarily on whole blood-derived DNA methylation data and are not expected to perform uniformly well across tissues. Therefore, if the cell-type composition of samples varied systematically across cohorts, this could produce differences in predictive accuracy that appear to be population-specific. We were especially concerned that the high frequency of the Duffy null variant in West African populations⁶¹, which is associated with lower neutrophil count in whole blood^{62–64}, could also drive ancestry-associated differences in saliva cell-type composition.

As expected⁶⁵, we found the Duffy null variant is fixed, or nearly fixed, in the Himba and Baka (allele frequency of 100% and 94%, respectively). The frequency of Duffy null in the ‡Khomani San cohort was 27%, consistent with gene flow from West African-ancestry populations in an environment where selection for malarial resistance is low⁶⁶. Because of the intermediate frequency of this allele in the ‡Khomani San and Baka cohorts, we were able to test for a relationship between Duffy null genotype and estimated neutrophil proportion, as well as with overall predictive accuracy. We applied a reference-based cell-type deconvolution method⁶⁷ to estimate cell-type proportions in each sample (see "Methods" section)⁶⁸. We observed a slight but non-significant negative relationship between neutrophil proportion and Duffy genotype in both the ‡Khomani San and Baka cohorts (Supplementary Fig. 4). However, we did not find that this led to a significant difference in prediction error across any of the 10 predictors (Supplementary Fig. 5).

Interestingly, there were fewer significant pairwise differences among cohorts across 10 different measures of epigenetic age acceleration (Supplementary Fig. 6). Most of these measures were derived from the Horvath¹², Hannum¹³, PhenoAge¹⁹, and GrimAge^{20,21} clocks, while one was developed independently as a DNA methylation-based estimate of the rate of telomere shortening⁶⁹ (see "Methods" section). Based on the PhenoAge and GrimAge-based epigenetic age acceleration metrics, the Himba and Baka both had significantly higher acceleration than the Hispanic samples for the former metric and higher acceleration than the European samples for the latter metric. In line with this, the Himba had significantly shorter methylation-based estimates of telomere length for their age than the Hispanic cohort, and the Baka had significantly shorter estimates of telomere

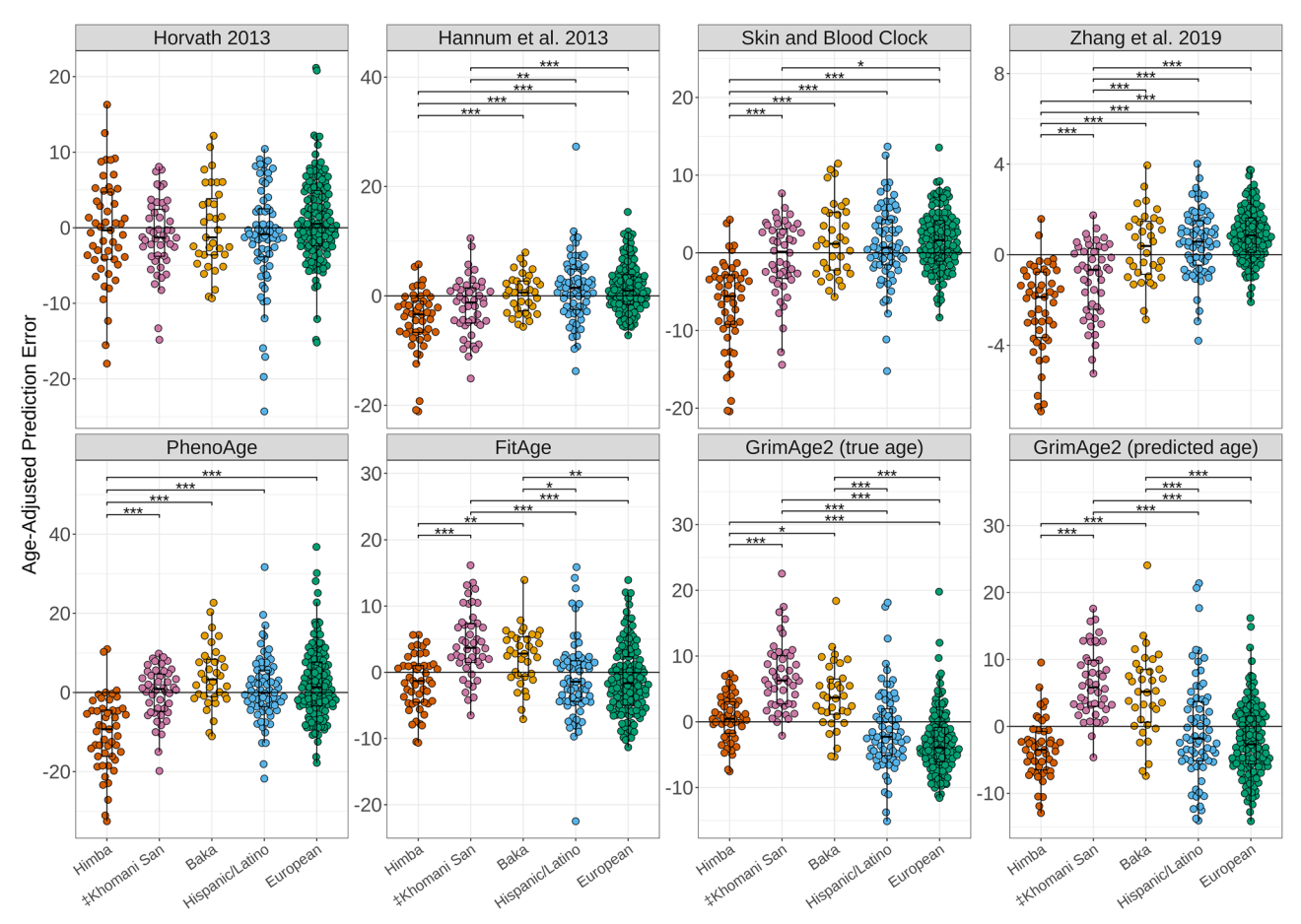


Fig. 1 | Distributions of age-adjusted prediction error across diverse cohorts. Beeswarm plots show differences in age prediction error for samples predicted to be saliva by dnamage.clockfoundation.org 90 , adjusted for individual age, among Himba (n=49), ‡Khomani San (n=46), Baka (n=35), Hispanic/Latino (n=69), and

European (n = 130) samples across 8 published epigenetic clocks. We tested for significant differences in age-adjusted prediction error among all populations by ANOVA, followed by a Tukey test to identify significant pairwise differences. * indicates an adjusted p-value of <0.05, ** <0.01, and *** <0.001.

length for their age than both the European and Hispanic cohorts (Supplementary Fig. 6).

Epigenome-wide association study for age

We conducted an epigenome-wide association study (EWAS) to identify CpG sites whose methylation levels are associated with age for each of our three population cohorts. We identified 347, 149, and 282 CpG sites that met the Bonferroni-corrected threshold for significance in the Himba, ‡Khomani San, and Baka, respectively, for a total of 567 unique sites (Supplementary Fig. 7A). 31 of these sites were identified independently in all three populations. We found that the estimated effect sizes were highly correlated in all three pairwise comparisons after conditioning on significance in at least 1 of the populations (Fig. 2A–C).

We next conducted a fixed-effect meta-analysis of our three populations to maximize our power to detect DNA methylation-age associations. Our meta-analysis identified 3211 significant age associations across the 355,103 CpG sites common to all three datasets (Fig. 2D). We found that 1637 of these overlapped with previously identified age-associated CpG sites identified in 34 published studies (Supplementary Table 3), including our previous study of the Baka and ‡Khomani San datasets⁷⁰.

Identification of cis-meQTL associations in African data

Next, we identified *cis*-meQTL that influence DNA methylation in our cohorts in order to understand the impact of nearby heritable variation on age-associated CpG sites. We conducted a 'baseline' *cis*-meQTL scan of each African cohort separately by testing a set of common, LD-pruned variants falling within 200 kb of each CpG site for association with DNA methylation

level (see "Methods" section). We identified 198,775, 75,120, and 61,525 significant meQTL in the Himba, ‡Khomani San, and Baka, respectively, affecting 11.7% (83,527), 11.1% (46,441), and 8% (32,167) of assayed CpG sites (Supplementary Fig. 7B). We then assessed the overlap of CpGs influenced by cis-meQTL and those whose DNA methylation levels are associated with age in our meta-analysis EWAS results. We found that 645 of the 3211 (20.1%) significant sites from the meta-analysis of the EWAS results are influenced by an meQTL identified in at least one population. Because our variant sets were different for each population and were LD pruned independently, the same SNP was rarely identified across multiple populations; however, we identified thousands of CpG sites that were influenced by meQTL in at least two populations (Supplementary Fig. 7B). In cases where the same SNP was identified as a significant meQTL we found that their effect sizes were very highly correlated across populations (Pearson correlations: Baka-‡Khomani San r = 0.97; Himba-‡Khomani San r = 0.96; Himba-Baka r = 0.97) (Fig. 3A).

We also conducted an 'extended' *cis*-meQTL analysis using the FUSION⁷¹ software package that considered a 1 Mb window around each CpG site to first estimate *cis*-heritability and then, for significantly heritable sites, model SNP weights using 4 regression methods: elastic net, LASSO⁷², SuSie (sum of single-effect)⁷³, and best single meQTL (see "Methods" section)⁷¹. We used non-LD-pruned genotype data for this analysis to gauge the extent to which the genetic architecture of CpG methylation is conserved across populations. We then moved forward with the best performing of the 4 regression models for each individual CpG site (Supplementary Table 4).

Even with our modest sample sizes, we found that a substantial proportion of CpG sites (6.7%, 8.2%, and 10.2% of CpGs tested in the Himba,

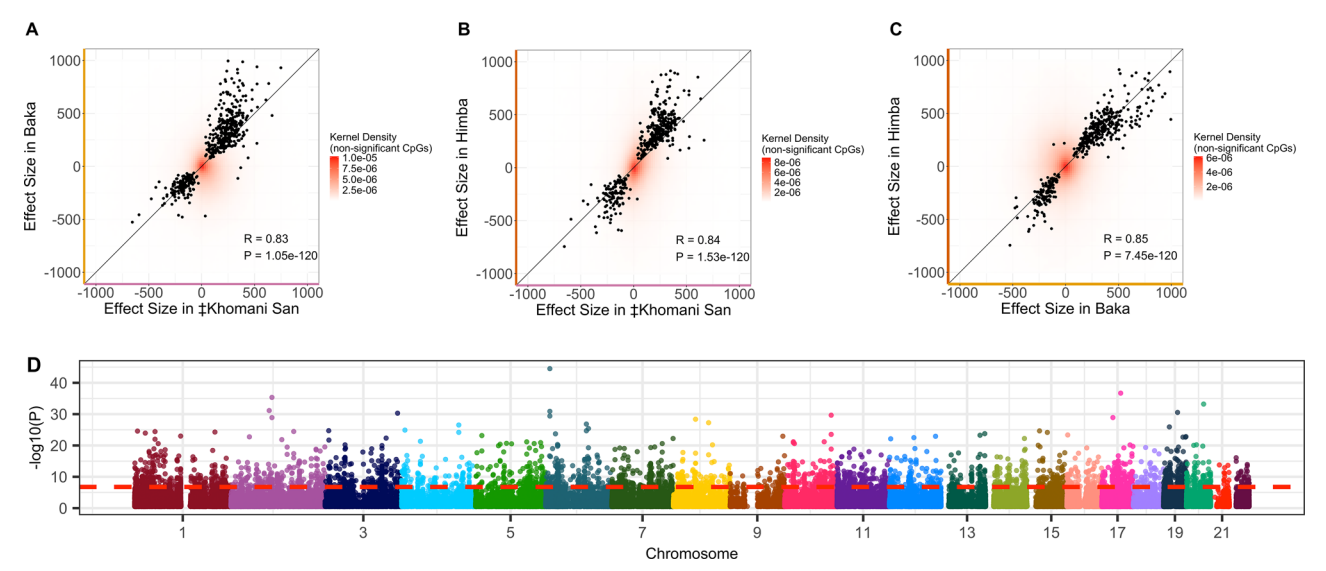


Fig. 2 | Strong correlation of epigenome-wide association effect sizes across populations. (A–C) show the correlation of estimated effect sizes of DNA methylation on age for all pairwise comparisons among the Himba (n=51), ‡Khomani San (n=52), and Baka (n=35). The black points indicate effect sizes for CpG sites that were significantly associated with age in at least one of the 3 populations. The red kernel density shows the distribution of effect sizes for CpG sites that were not significantly associated with age in any population. The Pearson correlation between effect sizes for the significant CpGs (black points) and the

significance of the correlation is indicated at the bottom right of each panel. (\mathbf{D}) is a Manhattan plot depicting associations between DNA methylation and age along the entire genome from a meta-analysis of the individual epigenome-wide association studies run in the three populations. A total of 3211 CpG sites exceed the threshold for significance, a p-value of 0.05 corrected for the number of CpG sites tested (red dotted line). Only non-significant effect sizes with an absolute value less than 1000 were included in the kernel density to restrict axes ranges for visualization purposes.

‡Khomani San, and Baka, respectively) exhibited significant cis-heritability (p < 0.05; Supplementary Fig. 7C). For these sites, *cis*-heritability of CpG methylation was significantly, but weakly, correlated across all pairs of populations (Pearson correlations: Baka-‡Khomani San r = 0.17; Himba-‡Khomani San r = 0.15; Himba-Baka r = 0.17) (Fig. 3D-F). We also tested the correlation of non-zero SNP weights from the FUSION⁷¹ models across population pairs, scaling weights within each regression model type, when the same SNP was reported to have a non-zero weight in multiple populations. We expected correlations to be lower than in the baseline meQTL scan, as different regression models could be selected as the bestperforming model across populations. Weights determined by the models allowing for joint cis-SNP effects (elastic net, LASSO, and SuSie) are dependent on the specific cis-variant sets in each population and would lead to lower correlations of weights across populations than correlating effect sizes from single variant models, which showed impressively high correlations (Fig. 3A). We did, however, still find moderately and significantly correlated non-zero SNP weights from the FUSION models (Pearson correlations: Baka-‡Khomani San r = 0.15; Himba-‡Khomani San r = 0.17; Himba-Baka r = 0.24) (Fig. 3G-I).

Accounting for *cis*-genetic influence in EWAS improves associations

Since meQTL variation is expected to add noise to the relationship between CpG methylation and age 13,70, we reasoned that regressing out SNP effects for significant meQTL from the corresponding DNA methylation values should improve age associations. To test this, we re-ran our population-specific EWAS after first regressing out the effect of the top meQTL genotype identified by our baseline scan from the respective CpG site's DNA methylation values. As expected, this approach resulted in a greater number of CpG sites passing the significance threshold compared to the original EWAS: 405 (increase of 58), 164 (increase of 15), and 312 (increase of 30), in the Himba, ‡Khomani San, and Baka, respectively (Supplementary Fig. 8A–F). This represents 751 unique sites identified across the three populations, an additional 96 sites compared to the original EWAS. 655 of the 657 original unique associations were replicated in at least one population in the meQTL-regressed EWAS.

We conducted a meta-analysis on the meQTL-regressed EWAS results and found 3,427 significant associations, including 224 CpG sites that were not significant in the original meta-EWAS (Supplementary Fig. 8G, H). 3203 of the 3211 associations identified in the initial meta-EWAS remained significant in the meQTL-regressed meta-EWAS. We found that for the 645 CpG sites that were significantly associated with age in the original meta-EWAS and also influenced by meQTL, 34.3% showed an improved association with age as reflected by a *p*-value reduction of at least one order of magnitude.

Across all CpG sites influenced by meQTL, 4.7%, 2.6%, 6.8%, and 2.4% improved their association with age by at least one order of magnitude in the Himba, ‡Khomani San, Baka, and meta-analysis, respectively (Fig. 4A–D). In order to ensure that this observed improvement was not spurious, we conducted a permutation analysis where we instead regressed out genotype values for a random SNP from a different chromosome. Across 100 permutations, only 0.03%, 0.08%, 0.06%, and 0.03% of CpG sites (Fig. 4A–D), on average, exhibited a similar magnitude of improvement, indicating that accounting for real meQTL associations does indeed improve our power to detect the relationship between CpG methylation and age (Fig. 4E–G).

cis-meQTL influencing popular epigenetic clocks are differentiated across populations

If meQTL influence a significant proportion of CpG sites used as predictors in epigenetic clocks, we would expect increased prediction error in population samples with divergent meQTL frequencies because predictor coefficients will be calibrated based on the average meQTL genotype of the training data. This would lead to particularly poor performance in out-of-sample prediction when an meQTL is very rare or invariant in the training data, but has common segregating variation in the target population. This is precisely the case in our study, as most published epigenetic clocks are trained on European-ancestry cohorts, but are being applied in African populations that have higher overall levels of heterozygosity⁷⁴.

We assessed the proportion of CpGs included in 6 of the published predictors that are influenced by meQTL identified in our baseline and extended scans; we excluded GrimAge and GrimAge2 as the details of these models are not publicly available. We found that between 22% and 43% of

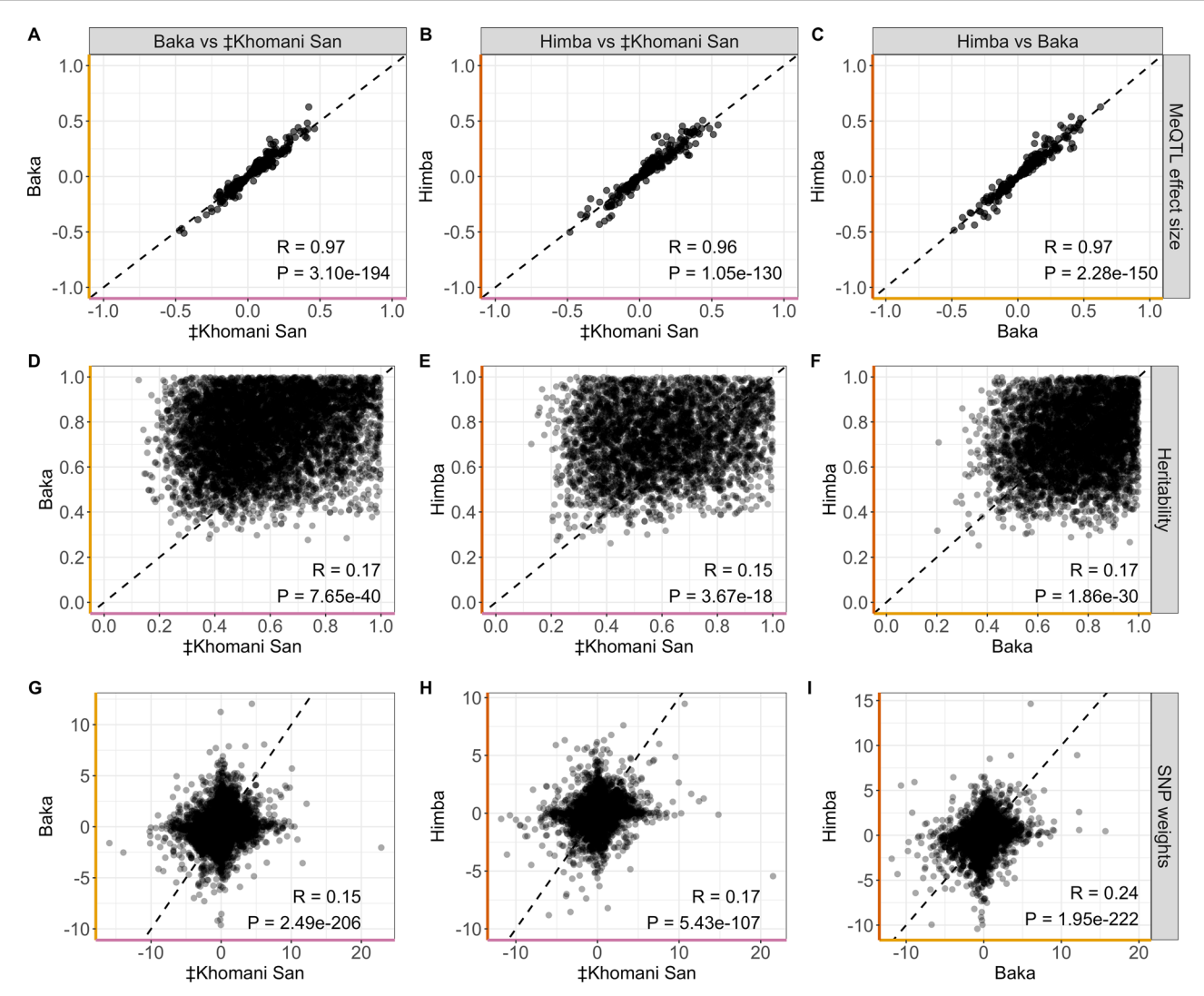


Fig. 3 | Shared *cis*-genetic architecture of CpG methylation among populations. (A–C) show the Pearson correlations of estimated effect sizes of SNP genotype on DNA methylation level from baseline *cis*-meQTL scans of the Himba (n = 51), ‡Khomani San (n = 52), and Baka (n = 35) for cases where the same SNP-CpG relationship was identified in both populations. (D–F) show the Pearson correlations in *cis*-heritability measures for significantly heritable (p-value < .05) CpG sites across all pairwise combinations of populations. (G–I) show the Pearson

correlations of *cis*-SNP weights on DNA methylation levels estimated from the FUSION regression models for the instances where the same SNP was estimated to have a non-zero weight across different populations, but the selected model was allowed to vary between populations. Weights were scaled within model type. In each panel, the dashed line represents the line of equality. The significance of the correlations is noted beneath the Pearson R values.

CpGs comprising the tested predictors are influenced by meQTL (Supplementary Data 1).

We next investigated meQTL allele frequencies in our 3 African populations and European populations from the 1000 Genomes Project⁷⁵ (Phase 3 European super-population, n = 2504 individuals). We limited this analysis to meQTL discovered from the baseline meQTL scans and aligned both 1000 Genomes and the African populations' reference and alternate alleles to match hg37. We found that the meQTLs influencing published epigenetic age predictors were often highly differentiated between European ancestry and our African populations (Fig. 5A-C). On average, these meQTL had a 10.6%, 13%, and 12.4% difference in frequency in the Himba, ‡Khomani San, and Baka compared to Europeans (mean F_{ST} of 0.11, 0.9, and 0.12, respectively). Importantly, 5.2%, 6.7%, and 9.2% of these meQTL are rare (<1% frequency) or invariant in Europeans, but common (>5% frequency) in the Himba, ‡Khomani San, and Baka. The CpGs influenced by these meQTL would show particularly poor relative performance in non-European samples in which these variants segregate at common frequencies (Fig. 5D-F, Supplementary Data 2). These proportions are likely an underestimate, as up to 3.5% of the meQTL we identify in the Himba,

‡Khomani San, and Baka were not present in the 1000 Genomes quality-controlled, biallelic variant set and could not be included in this analysis.

Epigenetic clock performance is improved by excluding the effects of heritable variation

Given that variation at meQTL can reduce power to detect age associations and that meQTL frequencies can vary substantially across human populations (Fig. 5A–C), it seems prudent to exclude CpG sites under known cisgenetic influence when developing epigenetic clocks; this should not only optimize within-cohort performance, but also out-of-cohort transferability. In order to test this hypothesis, we used elastic net regression to construct two types of epigenetic clocks using the combined data from all three African populations to maximize our power and reduce overfitting to any one population. Of the CpG sites common to the Himba, ‡Khomani San, Baka, and 4 out-of-cohort samples of different genetic ancestries, we allowed the elastic net regression to select either from 1) CpG sites without significant cis-heritability (not significantly influenced by a cis-meQTL and not significantly cis-heritable in any of the African populations, n = 213,689), or from 2) cis-heritable CpGs (significantly influenced by cis-meQTL or

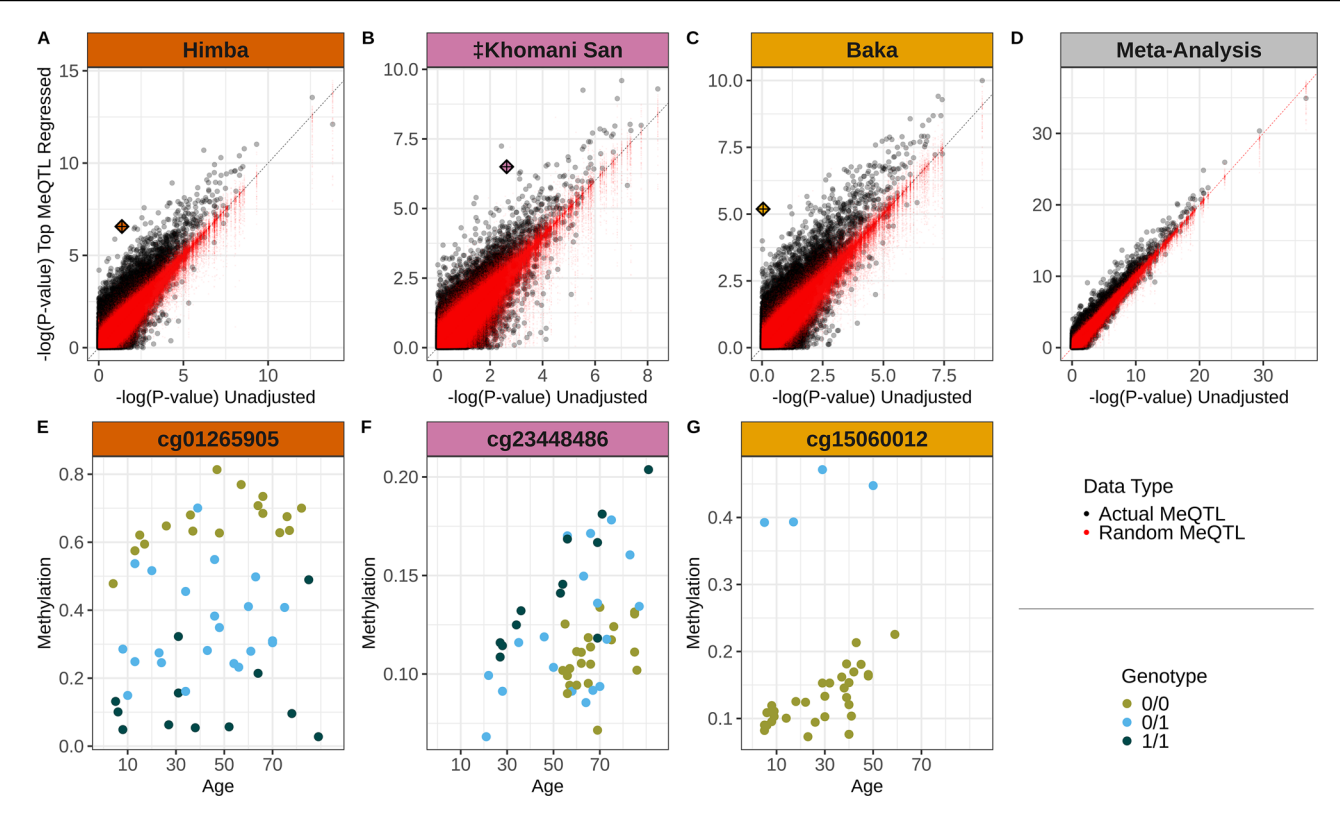


Fig. 4 | Accounting for meQTL genotype improves power to detect age associations. (A–D) show p-values for the association between CpG methylation and chronological age from the unadjusted epigenome-wide association study (x-axes) versus p-values from the meQTL-adjusted epigenome-wide association study (y-axes) in the Himba (n = 51), ‡Khomani San (n = 52), Baka (n = 35), and meta-analysis of the 3 populations. Red points show the results of 100 permutations where

a random SNP's genotype was regressed out rather than the true meQTL, whereas black points show the results from regressing out the true meQTL. (**E**-**G**) highlight the diamond points from (**A**-**C**), respectively, illustrating the influence of genotype on DNA methylation at CpG sites showing particularly large *p*-value improvements in the adjusted EWAS relative to the unadjusted EWAS.

determined to have significant *cis*-heritability in any of the 3 African populations, n = 116,132). We refer to these as our "non-heritable" and "heritable" epigenetic clocks, respectively.

Confirming the influence of meQTL in prediction transferability, we found that the non-heritable epigenetic clocks were more accurate than the heritable epigenetic clocks across 100 models, each tested on independent, held-out Himba, ‡Khomani San, and Baka test samples (Table 1). We next tested whether the non-heritable models would have better transferability across a diverse range of ancestries from tissue-matched samples. Supporting our hypothesis, the non-heritable models performed significantly better in the European- and Hispanic/Latino-ancestry cohorts as well as an additional Japanese cohort $(n = 19)^{76}$ (Table 1; Fig. 6). However, in an independent African-American cohort $(n = 64)^{77}$, both heritable and nonheritable clocks exhibited similar overall error (Table 1; Fig. 6). We speculate that this is due to our models failing to capture the full extent of meQTL diversity present in admixed African-Americans. Our epigenetic clocks exhibit predictive performance in African, European-ancestry, Hispanic/ Latino, African-American, and Japanese cohorts that is comparable to the reported test sample errors in the original Horvath and Hannum et al. publications^{12,13} (Table 1; Fig. 6). Overall, these results lend credence to the notion that heritable variation at meQTL negatively impacts both the transferability of epigenetic clocks as well as their overall predictive performance.

The combined effects of age-associated meQTL correlate with age and epigenetic age acceleration

Looking beyond age prediction, we wondered if meQTL variation at ageassociated CpG sites had biologically meaningful consequences for aging and longevity. To this end, we developed genotype-based epigenetic aging scores (EAS), which sum up the effects of meQTL variants on DNA methylation weighted by the effect of DNA methylation on age. EAS are analogous to polygenic scores that captures an individual genome's total burden of epigenetic age-elevating variants. For each cohort, we build an EAS model based on CpG sites that are both associated with age in that population's EWAS at a relaxed significance threshold (p < 0.001) and are significantly influenced by a *cis*-genetic variant in that population's baseline meQTL scan (see "Methods" section). Our ‡Khomani San model was based on 668 SNPs near 718 distinct CpGs, the Baka model on 987 SNPs near 1075 CpGs, and the Himba model on 1921 SNPs near 1995 CpGs. We then applied each of these models to genotype data from individuals within that cohort. Interestingly, we found that older individuals tended to have lower EAS, and consistently observed an overall negative relationship with age across all comparisons (Fig. 7A). Based on this observation, we hypothesize that having a lower burden of epigenetic age-elevating genetic variants might enable these individuals to achieve greater longevity.

Seeking additional evidence to evaluate this hypothesis, we compared these genotype-based EAS values with published measures of epigenetic age acceleration that are based solely on DNA methylation data ^{19,20,69,78}. These epigenetic age acceleration metrics have been shown to be associated with increased risk of multiple age-related conditions as well as all-cause mortality ^{15,78–80}. Interestingly, we found associations between EAS and several of these measures of biological aging or accelerated epigenetic aging; EAS trends towards being positively correlated with measures of 'intrinsic' and 'extrinsic' epigenetic age acceleration⁷⁸, while it trends towards being negatively correlated with an age-adjusted DNA methylation-based estimate of telomere length⁶⁹ (Fig. 7B–F, Supplementary Fig. 9). While not always significant, the trends we observe are consistently in the expected direction across populations and across acceleration metrics, supporting the role of genetic variants in influencing the pace of biological and epigenetic aging ^{12,13,56,81}.

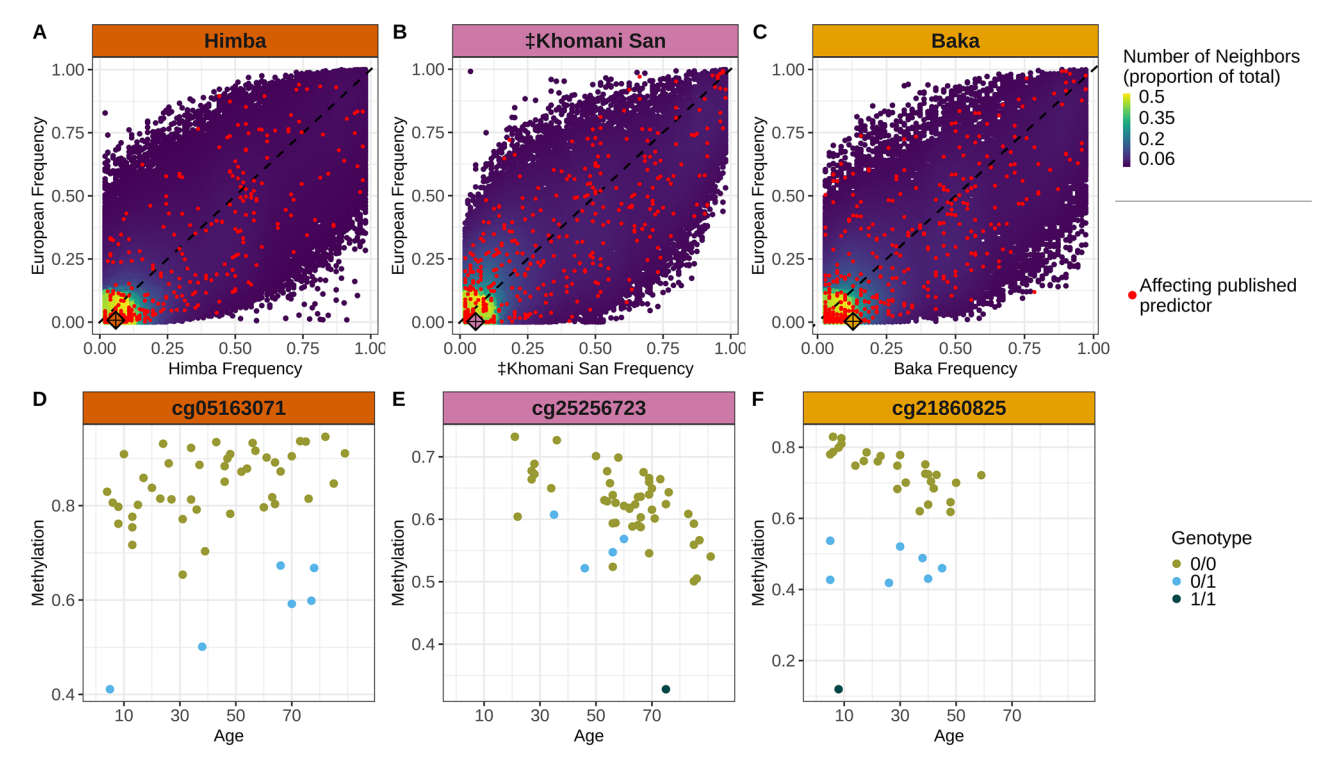


Fig. 5 | Differentiated meQTL influence CpG predictors in published epigenetic clocks. (A–C) show the allele frequencies of meQTL identified in each of the three African populations, Himba (n = 51), ‡Khomani San (n = 52), and Baka (n = 35), relative to their frequency in 1000 Genomes Phase 3 Europeans. The color of the points corresponds to the density of neighboring points, i.e, yellow points are in

high-density regions relative to dark blue points. Red points are meQTL influencing CpGs in published age prediction models. $(\mathbf{D}-\mathbf{F})$ show the influence of genotype on baseline methylation level for the meQTL highlighted with a diamond from the top row, examples of meQTL that are invariant in Europeans but segregate in the African population.

Table 1 | Mean absolute prediction error for the non-heritable and heritable epigenetic prediction models

	Heritable predictors error in years (SD)	Non-heritable predictors error in years (SD)	P-value of difference
African test samples	4.62 (.56)	4.25 (.56)	4.22e-06
European samples	5.87 (1.49)	5.03 (1.02)	6.29e-06
Hispanic/Latino samples	6.62 (1.17)	6.24 (1.14)	0.02
African-American samples	6.01 (1.23)	6.11 (1.78)	0.62
Japanese samples	5.94 (1.34)	4.53 (1.41)	1.09e-11

Mean absolute prediction error across 100 different models, each randomized for training and test splits. Standard deviations of the error distributions are listed in parentheses. Age predictors were trained on the combined African training samples using leave-one-out cross-validation and applied to held-out test samples. We applied these models to saliva-derived data from individuals of European, Hispanic/Latino, African-American, and Japanese ancestry. Non-heritable predictors were trained on the set of CpGs with no identifiable *cis*-meQTL associations and insignificant *cis*-heritablity. The heritable predictors were created from the complement set of CpGs, found to be either influenced by *cis*-meQTL or significantly *cis*-heritable. *P*-values are the results of a two-sided *T*-test comparing the non-heritable and heritable prediction error distributions. Mean raw prediction errors across all 100 models are listed in Supplementary Table 5.

Discussion

As a result of a growing interest in using epigenetic age predictors in clinical settings^{82–84}, models such as FitAge, PhenoAge, and GrimAge have been explicitly trained to capture traits such as maximal oxygen uptake (VO₂max), healthspan, and lifespan, respectively¹⁹⁻²². Epigenetic clocks intended for forensic applications, on the other hand, are concerned with accurately predicting an individual's chronological age, independent of lifestyle or overall health. However, regardless of the goals of any particular epigenetic clock, relatively little attention has been paid to the issue of transferability; i.e., how well a predictive model trained in one population or cohort performs when applied to another 40,85. Researchers have been grappling with an analogous issue in the development of polygenic risk scores (PRS), models that predict an individual's risk of complex disease based on their genotype. While initially heralded as a promising tool that would enable personalized genomic medicine, recent work demonstrates that applying PRS out-of-cohort can actually worsen health disparities due to poor transferability across human populations 45,86-88. Some of the underlying mechanisms that account for PRS's lack of generalizability, such as differences in allele frequencies and trait heritability across populations, may also be relevant for epigenetic clocks. In this work, we focused on discerning the influence of genetic factors on epigenetic clock transferability, but a loss of transferability could also be driven by variation in lifestyle or environmental factors across populations, which can directly impact DNA methylation patterns without perturbing the underlying DNA sequence

In testing several epigenetic clocks on three diverse African cohorts, we find that almost all exhibit significant among-population differences in prediction error, even after accounting for differences in data missingness, cohort age ranges, and potential tissue-predictor mismatch (see "Methods" section). Only the Horvath multi-tissue predictor showed no significant differences in age-adjusted error among cohorts (Fig. 1). This differs from previous results from our group and others that found that the Horvath multi-tissue predictor produces systematically different estimates for African-ancestry and Hispanic/Latino individuals compared to European-ancestry individuals^{34,36,70,89}. This discrepancy may be due in part to

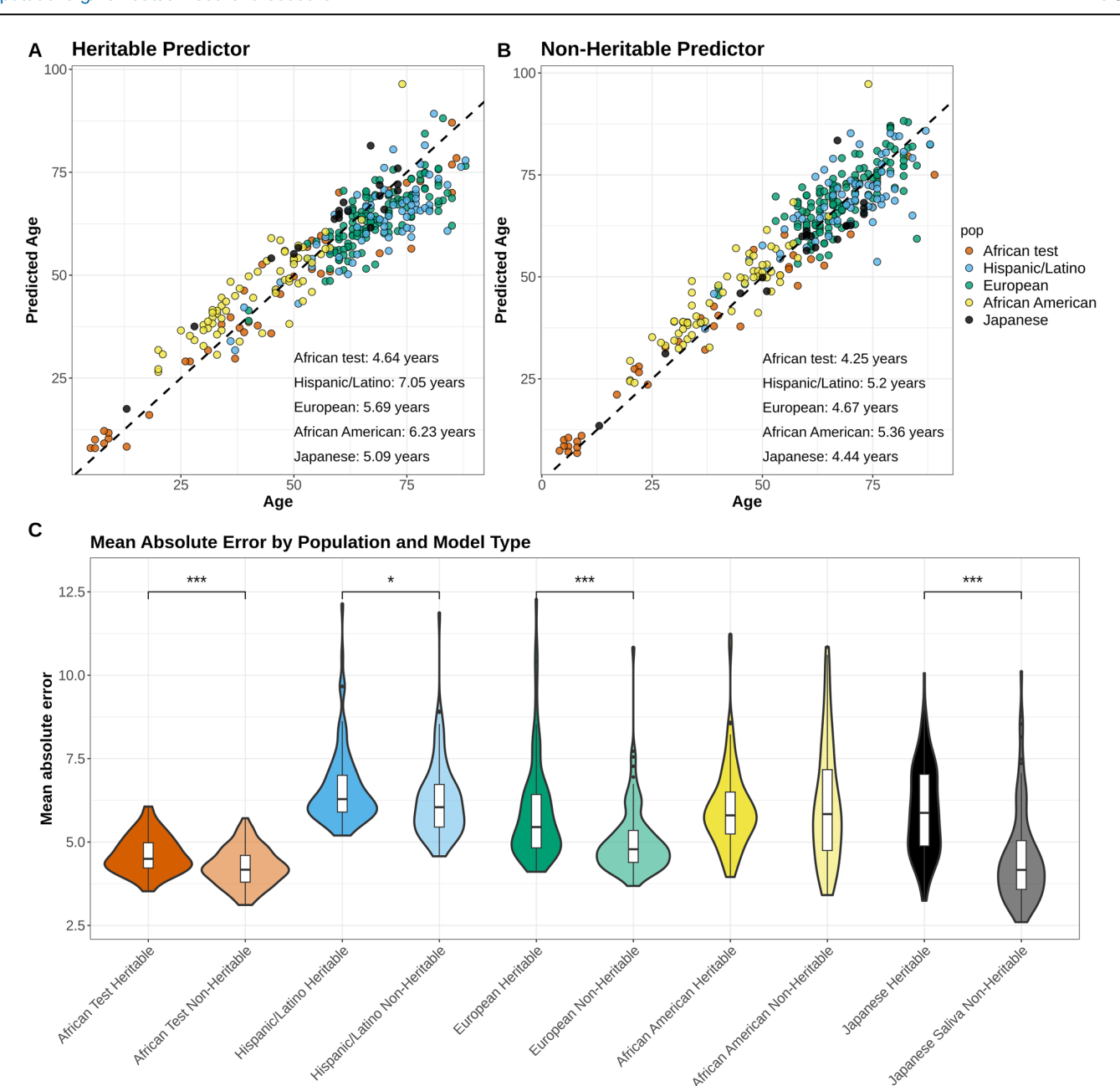


Fig. 6 | Performance of epigenetic clocks trained on heritable CpG sites versus non-heritable CpG sites. (A) and (B) are each based on a single model that exhibited the closest to the mean accuracy amongst the heritable models (A) or amongst the non-heritable models (B) in the African test samples (n = 44). (C) depicts the distributions of the mean absolute error from all 100 heritable and non-heritable models as applied to the African test subset (n = 44), Hispanic/Latino (n = 69), European (n = 130), African-American (n = 64), and Japanese (n = 19) cohorts. Boxplots depict the medians of the distributions and the $1.5 \times$ interquartile ranges.

Models based on CpG predictors that are not significantly impacted by *cis*-genetic variation exhibit lower absolute error and less bias when applied to our test samples and to out-of-cohort samples than models based on CpG sites that are significantly heritable, except for when applied to the African-American samples. Table 1 shows the mean absolute values and standard deviations of each of the distributions in panel C and exact *p*-values of the two-sided *T*-tests. * indicates a *p*-value of <0.05, ** <0.01, and *** <0.001.

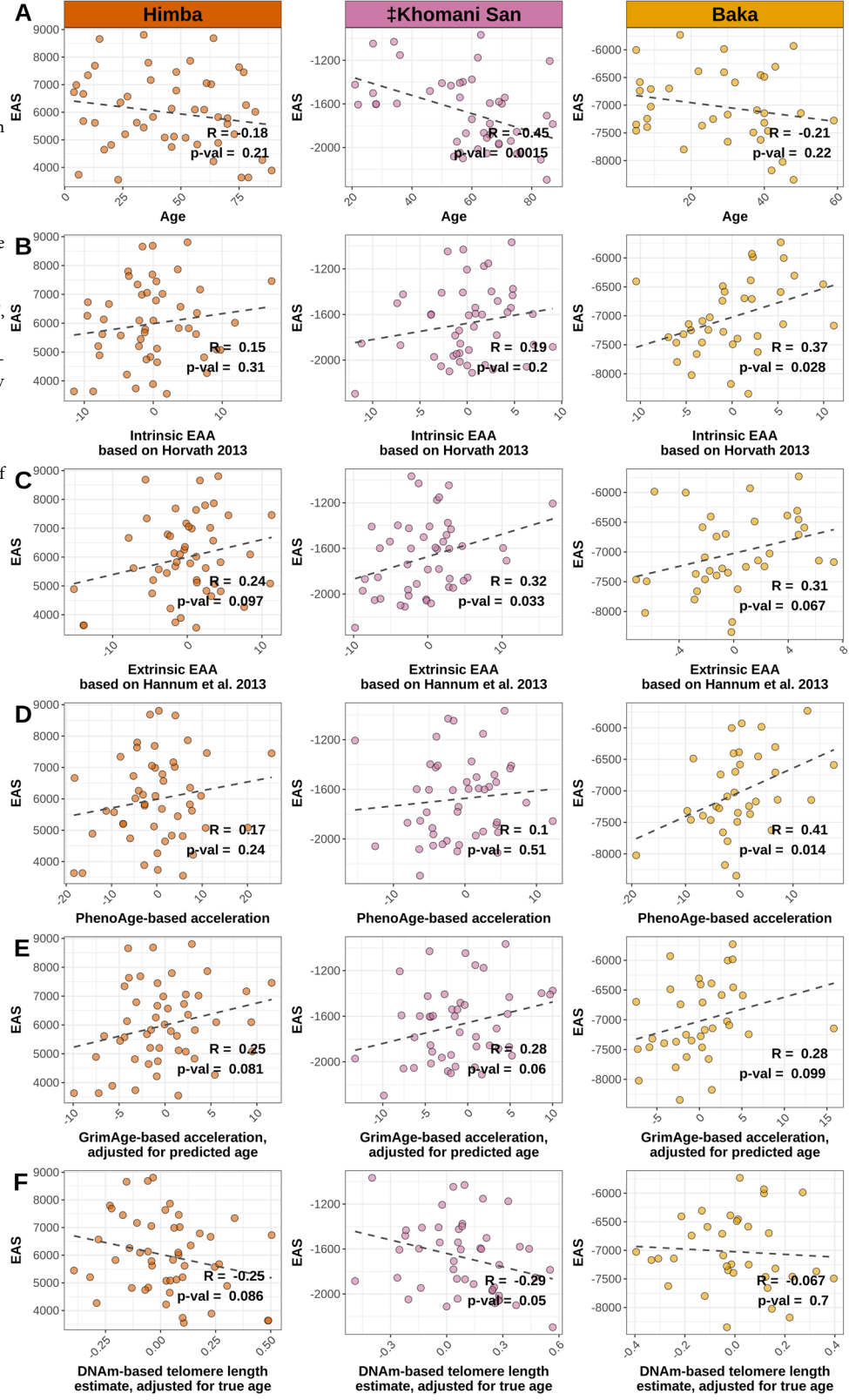
differences in implementation; in our prior work, we applied the Horvath algorithm to quality control filtered DNA methylation values that had been pre-normalized and imputed⁷⁰, whereas here it was applied to raw and unfiltered data according to the online platform standards (see dnamage.clockfoundation.org⁹⁰). This highlights an additional issue impacting transferability, namely a lack of agreed-upon best practices for DNA methylation data processing and quality control.

Unlike previous work, we also did not find any significant differences among populations for any of the epigenetic age acceleration metrics derived from the Horvath and Hannum clocks ^{19,31–34} (Supplementary Fig. 6). It has been suggested that apparent among-population variations in

epigenetic age acceleration could indicate, or help explain, real differences in the average health and/or longevity of different human groups ^{19,24,31-34}. However, contradictory results across clocks and across studies, along with decreasing chronological age prediction accuracy in genetically diverged samples, suggest underlying issues in clock transferability ^{19,31-33,41-43,91}. Since most epigenetic clocks have been trained primarily on European-ancestry individuals living in industrialized societies, we instead suggest that these discrepancies might be partially explained by differential transferability across populations.

Although we did not have the health and mortality data required to rigorously evaluate the relationship between epigenetic age acceleration and

Fig. 7 | Relationship between epigenetic aging score (EAS) and aging metrics. Scatterplots show the relationship between the genotype-based epigenetic aging score (EAS) and various metrics of epigenetic age acceleration for the Himba, ≠Khomani San, and Baka. Each EAS model was built from the respective population's epigenome-wide association study and baseline meQTL scan results. Individuals' EAS values were plotted against A chronological age itself, B 'Intrinsic Epigenetic Age Acceleration' based on the Horvath multi-tissue **B** 9000 age predictor78, C 'Extrinsic Epigenetic Age Acceleration' based on the Hannum predictor⁷⁸, D epigenetic age acceleration based on PhenoAge¹ E epigenetic age acceleration based on GrimAge²⁰, adjusted for predicted age, and F DNA methylationbased telomere length69, adjusted for true age. Only samples predicted to be saliva or blood from the online platform were used: Himba (n = 49), ‡Khomani San (n = 46), Baka (n = 35). Pearson correlations and unadjusted *p*-values for the significance of the correlation are shown in the bottom right of each panel.



health outcomes in the Himba, ‡Khomani San, and Baka, our results demonstrate that poor transferability across ancestries should be considered as a possible explanation for among-population differences. For example, we found that PhenoAge and GrimAge2 exhibited qualitatively different patterns in our among-population comparisons, even though both of these epigenetic clocks were designed to capture signatures of age-associated morbidity and mortality (Fig. 1). Although these clocks were designed to

capture slightly different aspects of the aging phenotype, we would not expect these kinds of inconsistencies if Himba individuals are truly aging faster (or slower) on an epigenetic level compared to European-ancestry individuals.

Furthermore, we find that common genetic variation is a significant factor affecting age association and epigenetic clock performance. We recover hundreds of age associations after accounting for meQTL genotype

and find that all of the published epigenetic clocks include CpG predictors that are impacted by cis-genetic variation. Furthermore, a substantial fraction of this variation is rare or absent in European-ancestry populations. Populations that experienced the out-of-Africa migration bottleneck carry only a subset of the genetic variation that exists in African populations⁹²; therefore, we expect that our analyses capture a majority of the meQTL variation that exists in the European, Hispanic/Latino, and Japanese ancestry cohorts. In training our own epigenetic clocks, we show that excluding CpG sites with detectable cis-heritability improves prediction accuracy and reduces bias when applied to these out-of-Africa ancestry populations relative to clocks that only include heritable CpG predictors (Table 1, Fig. 6). However, we found no difference in prediction accuracy between the heritable and non-heritable predictors when applied to the African-American sample. This suggests that our approach still does not adequately account for the full range of meQTL diversity that segregates in this population and/or that recent admixture introduces additional challenges. Therefore, future work should continue to expand the diversity of training and validation samples across multiple tissue types with a particular focus on African-ancestry and recently admixed populations.

Until we have a better understanding of the genetic architecture of DNA methylation variation across diverse human populations, training predictors on minimally heritable CpG sites is a straightforward and effective approach to improving transferability. This is particularly true for forensic applications, where generating an accurate estimate of chronological age regardless of health status is the primary goal. However, given the remarkably strong correlation of meQTL effect sizes across genetically diverged populations (Fig. 3A–C), future epigenetic clocks could see even greater improvements by explicitly accounting for individual genetic variation. Therefore, while environmental differences could still drive variation in DNA methylation, and thus prediction error, across cohorts, we show that heritable factors play a significant role in transferability across cohorts.

Although we refer to the difference between individual chronological age and predicted age as 'prediction error' throughout this paper, it must be noted that these deviations are not necessarily true errors; for some epigenetic clocks, these deviations do appear to reflect meaningful variation in human health, morbidity, and/or mortality within specific populations^{82–84}. However, as we have outlined above, it is not clear to what degree amongpopulation differences in mean estimates are indicative of genuine variation in the rate at which different human populations age, versus a simple lack of transferability. Answering this question will require a complete understanding of the connections between various genetic, environmental, and lifestyle factors and CpG methylation, as well as their interactions and downstream effects on the aging phenotype. Our work here focuses on the genetic factors, whose effects on CpG methylation we are able to dissect by jointly analyzing DNA methylation and genotype data. Additionally, our multi-population study design enables us to characterize the extent to which the genetic architecture of age-associated CpG methylation is shared across diverse genetic backgrounds and environments (Fig. 3). As our phenotypic data was limited to chronological age, we demonstrate that accounting for heritable CpG sites can improve chronological age prediction but we cannot directly assess improvement to biological age/morbidity predictors. However, based on our results, we would expect biological age/morbidity predictors to likewise benefit from excluding heritable CpG sites.

We were also able to investigate the potential impact of genetic variation on the aging phenotype by developing an epigenetic aging score (EAS) that reflects the cumulative effect of meQTL variants that influence age-associated CpGs. We find suggestive evidence that our EAS is associated with older chronological age and with epigenetic age acceleration in these populations (Fig. 7). If genetic factors influence lifespan and healthspan, we might expect that older individuals will have lower EAS (i.e., a lower burden of epigenetic age-increasing variants) while younger individuals will exhibit a wider range of EAS values. In our data, we find that this pattern manifests as a slight negative correlation between EAS and chronological age. Furthermore, we find that EAS is also correlated with various estimates of epigenetic age acceleration, despite the fact that these metrics were not

trained on African populations and thus are likely underpowered. Although not always significant, the consistency of these associations in the expected direction is nevertheless compelling. These results also corroborate previous work that has found that both healthspan and lifespan are heritable, polygenic traits^{12,13,56,81,93}. In his 2013 paper, Horvath noted 21 genes that carried common variants associated with increased epigenetic age in his multitissue clock. Interestingly, six of these genes (FAM123C, LEPR, CHD7, CTNND2, TMEM132D, and MACF1) were proximal to a CpG site included in at least one of our population-specific EAS models. These results suggest that our EAS models are picking up on real signals of a genetic predisposition to accelerated biological aging within these African populations that warrant further investigation. Within-population heterogeneity in environment and lifestyle factors such as diet⁹⁴ and infectious disease burden^{95,96} would reduce our power to detect the influence of genetic sequence variation on methylation. However, despite these challenges and our low sample sizes, we believe our study is particularly well-suited to identify these signals. Relative to industrialized populations, amongindividual variation in socioeconomic status, diet, and other lifestyle factors is relatively low within our cohorts, as samples were collected within small communities by walking from house to house (see "Methods"

The extent to which the pace of epigenetic aging is determined and modulated by heritable versus non-heritable factors is still very much an open question, with important implications for the problem of transferability. These issues must be carefully considered as epigenetic clocks are being more frequently applied in contexts where these genetic and environmental factors are often confounded. For example, the relatively new subfield of 'social epigenomics' seeks to understand how socioeconomic and environmental factors influence DNA methylation and drive health disparities in cosmopolitan populations²⁴. Differences in epigenetic age acceleration among racial and/or ethnic groups are typically interpreted as arising from systemic differences in socioeconomic status, etc. However, it is possible that poor model transferability partially accounts for these observations. This alternative explanation does not minimize the growing body of evidence that broadly demonstrates that various social determinants of health, such as psychosocial stress⁹⁷, diet⁹⁴, and smoking behavior⁹⁸, influence DNA methylation. Rather, we caution that genetic ancestry should be more carefully considered in studies of epigenetic aging and its consequences for human health, as it is often confounded with underserved minority status, particularly in the Global North.

Methods

Sample collection

Saliva samples from 3 different African populations were collected between 2006 and 2016 using Oragene DNA self-collection kits. 51 Himba individuals (aged 4–89, median age 46; 28 females and 23 males), $52 \neq$ Khomani San individuals (aged 21–91, median age 62.5; 33 females and 19 males), and 35 Baka individuals (aged 5–59, median age 30; 19 females and 16 males) had paired DNA methylation and genotype data that passed quality control. The Baka dataset comprises nine trios and nine unrelated individuals. The data from the \neq Khomani San and Baka individuals have been previously analyzed⁷⁰.

Population descriptions

The three populations included here occupy very different geographic locales and have varied subsistence strategies. The Himba are a Bantuspeaking agropastoralist population living on the northern border of Namibia. Their environment is a semi-arid mopane woodland with seasonal creeks and a perennial river to the north. About 30,000-40,000⁹⁹ people belong to the Himba ethnic group, which has maintained traditional dress, subsistence, and domicile to a greater extent than the closely related Herero. Today, their diet consists mainly of meat and sour milk from their cattle and goats in combination with maize, melon, and other vegetables grown in their gardens. While social status is marked by the size of their herds, dietary diversity varies little among families. Drought periodically affects northern

Namibia, resulting in cattle loss⁹⁹; in such instances, the Himba typically supplement with store-bought items and report moderate food insecurity¹⁰⁰.

The ≠Khomani San are a formerly hunter-gatherer population in the southern Kalahari Desert. While some elders grew up foraging, most people in the study are now wage laborers on sheep farms, receive government subsistence, or rely on remittances from relatives in larger towns. The population is primarily sedentary in very small towns or farms in the region. Due to their limited income, diet is a mix of purchased goods (flour, potatoes, maize, cabbage, etc.) for stews or baked bread, and meat from local farms (generally sheep/goat, but also donkey and cattle). Gathering 'wild food' continues to supplement their diet. Many families report nutritional stress' (personal communication, BMH).

The Baka are a foraging-horticulturalist population from southeastern Cameroon and Gabon, living in the central African rainforest. Due to their economic relationships with Bantu-speaking farmers and encroachment into the rainforest, the Baka have been increasingly residing in sedentary villages within forest clearings. Starchy foods such as cassava, wild yams, and plantains are staples to which leafy greens and hunted meat and fish are added. Wild herbs, mushrooms, and nuts also require frequent effort to obtain from nearby forests¹⁰². Many families are resource-limited, having only one main meal a day.

DNA methylation microarray quality control and filtering

DNA was bisulfite converted, whole-genome amplified, fragmented, and hybridized to the Illumina Infinium HumanMethylation450 (>485,000 CpG sites) BeadChip array for the Baka and ‡Khomani San samples and the EPIC Array (>845,000 CpG sites) for the Himba samples. DNA methylation array data was generated in 4 batches, with both the ‡Khomani San and Himba samples separated across two batches (Supplementary Table 6). One ‡Khomani San individual was typed in both batches, and two Baka individuals were typed twice in the same batch. The overall intra-class correlations between DNA methylation values for these 3 sets of replicates were 0.9985, 0.9991, and 0.9989, respectively. One Himba individual, sampled three years apart, was typed across the two Himba batches. The overall intraclass correlation between methylation values from this individual was 0.9974, lower than for a purely technical replicate, as expected. Only the earlier sample from this individual was used in the EWAS and meQTL analyses. One Baka individual was flagged for having abnormally low bisulfite controls and removed from analyses.

We removed DNA methylation probes with a detection p-value > 0.01 in greater than 5% of samples, as well as any probes that have been reported to be cross-reactive, map to multiple regions, or to the sex chromosomes 103,104 (Supplementary Table 7). Any remaining values with detection p-values > 0.01 were set to NA. We also removed CpG sites that were likely to be impacted by SNPs in or near the probe sequence in a population-specific manner using our published software, probeSNPffer (https://github.com/ gillianmeeks/probeSNPffer)^{105,106}. Specifically, we retrieved the hg19 genomic coordinate of the target cytosine for each DNA methylation array probe and searched the full 50 base pair probe region, the next base extension (for type 1 probes), and the extension base (for type 2 probes) for overlap with SNPs segregating at >5% frequency in a given population 105. SNPs within array probes can lead to reduced probe hybridization efficiency and unreliable methylation signal 103,105,107. An additional 27,242, 9254, and 61,662 probes were pruned from the Baka, merged ‡Khomani San, and merged Himba DNA methylation datasets, respectively, from this step.

After these filtering steps, we were left with 713,988 CpG sites in the Himba dataset, 418,629 sites in the ‡Khomani San dataset, and 400,893 sites in the Baka dataset. There was an overlap of 355,103 sites across all three populations that we used for the combined analyses. DNA methylation values were background and color corrected, and technical differences between type 1 and type 2 probes were corrected by performing BMIQ normalization using the wateRmelon¹⁰⁸ and minfi¹⁰⁹ R packages. All analyses were performed using continuous DNA methylation beta values for each CpG site, which range from 0 (indicating that the site is completely unmethylated) to 1 (completely methylated).

Genotype data quality control and filtering

Genotype data was generated using multiple arrays for the ‡Khomani San and Himba samples, while the 35 Baka individuals were all genotyped on the Illumina OmniOne array. All genotype data were oriented to match the 1000 genomes Phase 3 GRCh37 reference, filtered to exclude SNPs with a genotype missing rate >5%, minor allele frequency of <1%, and Hardy-Weinberg deviation *p*-value < 0.0001. We removed all indels and A/T or C/G transversion variants. Sample sizes and pre-imputation variant counts are listed in Supplementary Table 8. Principal components analysis of the three populations' genotype data is shown in Supplementary Fig. 10.

Each genotype array dataset was phased using SHAPEITv2.r790¹¹⁰ and imputed using the Positional Burrows-Wheeler Transformation (PWB)¹¹¹ to the African Genomics Resources Panel (89,838,088 autosomal variants, 4956 samples) via the Sanger Imputation Service⁵⁷. We assessed imputation accuracy in our samples by calculating imputed genotype concordance with sequencing data. For the ‡Khomani San, we compared imputed genotypes with whole-exome sequence data for 37 individuals. The overall concordance with the ‡Khomani San exome variants was 95.7%-97.7% across the genotype arrays for variants of any impute quality INFO score (Supplementary Fig. 11D). For the Himba, we compared genotypes imputed from MEGAex array data with genotype calls uniquely typed on the H3Africa array data for 3 Himba individuals genotyped on both platforms. The average concordance of imputed H3Africa SNPs was 98% for the 3 Himba individuals typed on both H3Africa and MEGAex (Supplementary Fig. 12D). We also stratified concordance by imputed quality INFO score, and observed 99% concordance across all genotype arrays in the ‡Khomani San and Himba at a >0.95 INFO score (Supplementary Fig. 11D, 12D). This observation informed our choice to only retain imputed variants with >0.95 INFO score for subsequent analyses. Imputed data from OmniExpress and MEGAex arrays performed slightly better on concordance metrics for all INFO score bins than the 550K array (Supplementary Fig. 11A-D), most likely due to denser genotyping, so genotype data from these arrays were used for the 17 ‡Khomani San individuals typed on multiple arrays. After filtering and merging across genotype arrays, we retained 66,484,843 highquality autosomal variants for the ‡Khomani San, 78,738,543 for the Himba, and 75,739,815 for the Baka.

Epigenome-wide association studies (EWAS)

We used EMMAX¹¹² with the dosage option to test for the association between age and methylation level separately in each population, accounting for population-specific, scaled covariates and a Balding-Nichols kinship matrix (Eqs. 1–3).

DNA methylation array data are known to exhibit significant batch effects; that is, samples on one run vary systematically from samples on another due to technical artifacts. We controlled for DNA methylation array batch effects by including the first 20 PCs of control probe intensities 113 as covariates in the EWAS for the Himba (Eq. 1). Regressing out these control probe PCs eliminates batch effects in the first two methylation PCs (Supplementary Fig. 13C, D). We did not have access to the raw intensities for the Baka and ‡Khomani San methylation datasets, so we controlled for technical artifacts by including batch number as a covariate in ‡Khomani San where samples were split across batches (Supplementary Fig. 13A, B). To control for technical artifacts present within a batch, we included the combination of the first 5 DNA methylation PCs that we found best reduced genomic inflation. We did not include all of the first 5 methylation PCs as covariates to mitigate power loss, as up to one third of the methylome has been found to show association with age¹.

We included sex and the first 5 genetic PCs as covariates in all models (Eqs. 1–3). We computed the latter using LD-pruned (PLINK1.9⁷² --indeppairwise 50 5 0.3) variants above 5% frequency within each population. There was no evidence of clustering based on genotype array in the ‡Khomani San (Supplementary Fig. 10A). We estimated cell-type proportions using the R package EpiDish⁶⁷, leveraging DNA methylation data from a reference panel of 12 different blood cell types, epithelial cells, and fibroblast cells. The proportions estimated by this method correspond

closely to previous estimates of saliva cell composition ⁶⁸ (Supplementary Fig. 14). As neutrophils and epithelial cells together account for nearly 100% of the cells in our saliva samples, we included just the neutrophil proportion as an additional covariate in our models. Cell-type proportion estimates for the replicate samples were highly similar (Supplementary Table 9). We compared our reference-based deconvolution approach to reference-free estimates of cell-type proportions using the TOAST¹¹⁴ R package. Under a k=2 cluster model, the correlation with the reference-based neutrophil and epithelial cell proportion estimates was 0.98.

Himba Age = Intercept +
$$\beta_{Methylation\%} + \beta_{Ctrl\ Probe\ PCs1-20}$$

+ $\beta_{Genetic\ PCs1-5} + \beta_{Neutrophil\%} + \beta_{Sex} + \beta_{BN\ kinship\ matrix}$ (1)

‡Khomani San Age = Intercept +
$$\beta_{Methylation}$$
 % + β_{Batch}
+ $\beta_{Methylation}$ PCs1,3 + $\beta_{Genetic}$ PCs1-5
+ $\beta_{Neutrophil}$ % + β_{Sex} + β_{BN} kinship matrix

Baka Age = Intercept +
$$\beta_{Methylation \%}$$
 + $\beta_{Methylation PCs2,3}$
+ $\beta_{Genetic PCs1-5}$ + $\beta_{Neutrophil \%}$ + β_{Sex} + $\beta_{BN kinship matrix}$ (3)

We used the metagen¹¹⁵ R software package to conduct a fixed-effect meta-analysis of our EWAS results from all three populations. Significance was determined at a Bonferroni-corrected *p*-value of 0.05, correcting for the number of overlapping CpGs across the three populations. We set the Hartung and Knapp adjustment to false and the between-study variance method to REML.

Baseline cis-meQTL scan

We used EMMAX¹¹² with DNA methylation value as the dependent variable to identify *cis*-variants that are significantly associated with DNA methylation levels at each CpG site. SNPs with a minor allele count of less than 2 were removed to leave 2,432,803 for the ‡Khomani San, 6,594,680 for the Himba, and 4,944,508 for the Baka. We performed within-population *cis*-meQTL scans using LD-pruned genotype datasets (generated using the PLINK1.9⁷² option --indep-pairwise 50 5 0.5) by testing each SNP within a 200 kb window (100 kb upstream and downstream) of the target CpG for association with DNA methylation level. The same population-specific scaled covariates as in the EWAS scan were used with age as an additional covariate (Eqs. 4–6). We determined significance at a *p*-value of 0.05 corrected for the number of SNPs tested at each CpG.

$$\begin{split} \textit{CpG}_{\textit{i},\textit{Himba}} &= \textit{Intercept} + \beta_{\textit{cis-genotype}}\,_{(0/1/2)} + \beta_{\textit{Ctrl Probe PCs1-20}} \\ &+ \beta_{\textit{Genetic PCs1-5}} + \beta_{\textit{Neutrophil}}\,_{\%} + \beta_{\textit{Sex}} + \beta_{\textit{BN kinship matrix}} + \beta_{\textit{Age}} \end{split}$$

$$CpG_{i, \ddagger Khomani San} = Intercept + \beta_{cis-genotype (0/1/2)} + \beta_{Batch}$$

$$+ \beta_{Methylation PCs1,3} + \beta_{Genetic PCs1-5} + \beta_{Neutrophil \%}$$

$$+ \beta_{Sex} + \beta_{BN kinship matrix} + \beta_{Age}$$
(5)

$$CpG_{i,Baka} = Intercept + \beta_{cis-genotype (0/1/2)} + \beta_{Methylation PCs2,3}$$

$$+ \beta_{Genetic PCs1-5} + \beta_{Neutrophil} \% + \beta_{Sex} + \beta_{BN \ kinship \ matrix} + \beta_{Age}$$
(6)

Heritability of CpG methylation

We estimated *cis*-heritability of DNA methylation at each CpG site using GCTA¹¹⁶ within FUSION⁷¹ and default parameters (--reml --reml-no-constrain --reml-lrt 1). We tested a 1 Mb window (i.e., 500 kb upstream and downstream) around each CpG site. We used the same genetic datasets as

used in the baseline meQTL scan prior to the LD pruning step. The same covariates were used as in the baseline meQTL scans (Eqs. 4–6).

FUSION cis-meQTL scan

We modified functions from the FUSION⁷¹ software package, originally designed to uncover the *cis*-genetic architecture of gene expression, to test elastic net, LASSO⁷², SuSie (sum of single-effect)⁷³, and the best single meQTL regression models to explain methylation levels at each CpG site. The former 3 regression models allow for multiple SNP effects to jointly influence methylation rather than testing the effect of each SNP independently, as in our baseline scan. Only CpGs with significant (p-value < 0.05) cis-heritabilty were modeled using the 4 regression models. The FUSION framework conducts 5-fold cross-validation analyses to select the regression model that yields the highest R-squared in explaining cis-genetic variation's effect on DNA methylation and stores the effect sizes (i.e., weights) associated with each variant under each model.

MeQTL-adjusted EWAS

We re-ran our EWAS (Eqs. 1–3), this time testing for age associations with the residual values after regressing out the top meQTL genotypes from respective CpG's methylation values. For instances of multiple significant meQTL influences a CpG, we choose the variant with the lowest *p*-value. This was done for each CpG site with a significant meQTL association. We used the same covariates as in the original EWAS (Eqs. 1–3).

Testing published epigenetic clocks

We tested all 10 published age predictors available through the Clock Foundation online portal at dnamage.clockfoundation.org⁹⁰. The Horvath¹², Hannum¹³, skin and blood⁵⁸, and Zhang elastic net⁵⁹ clocks are all chronological age predictors built using penalized linear regression. The PhenoAge¹⁹, GrimAge²⁰, GrimAge²¹, and Fitage²² clocks are built on CpGs associated with surrogate measures of biological age, capturing variables that predict lifespan, healthspan, and mortality risk. GrimAge and GrimAge2 models incorporate chronological age within their surrogate measure and can be constructed using actual chronological age (GrimAge on true age) or using estimates of chronological age from the skin and blood clock predictor⁵⁸(GrimAge on predicted age). See eTable 1 in Krieger et al. ³⁰ for detailed descriptions of each predictor. The Horvath¹² multi-tissue clock was trained on data from 51 different tissue types, specifically designed to be a pan-tissue predictor. The skin and blood⁵⁸ clock was trained on data derived from fibroblasts, keratinocytes, buccal cells, endothelial cells, lymphoblastoid cells, skin, blood, and saliva samples. The Zhang elastic net⁵⁹ clock was trained on data derived primarily from whole blood samples, with 2% from saliva-derived data. The other predictors were trained on whole bloodderived samples.

Each model's age predictions are a weighted sum of an individual's DNA methylation values at the predictor CpG sites, and are thus very sensitive to missing data. Therefore, in order to fairly compare predictions across populations, and in accordance with recommendations published with the online tool, we uploaded raw, unfiltered beta values for each individual. Additionally, we restricted our dataset to CpG sites that were common to all three African populations and the European and Hispanic/ Latino datasets. In addition to estimates of epigenetic age from the different prediction algorithms, the Clock Foundation online portal⁹⁰ performs a host of quality control analyses based on the input DNA methylation values, including tissue type prediction using an unpublished algorithm. We compared EpiDish⁶⁷ estimated cell-type proportions across the predicted tissue types and found samples predicted to be saliva, blood PBMC, or whole blood and found cell-type proportions were essentially indistinguishable in our dataset (Supplementary Fig. 14). We conservatively excluded samples predicted to originate from tissue types other than saliva, blood PBMC, or whole blood, resulting in the following final sample sizes for these clock validation analyses: Himba (n = 49; median age 47, age range 4–89; 28 females and 21 males), \ddagger Khomani San (n = 46; median age 62, age range 21–87; 31 females and 15 males), Baka (n = 35; median age 30, age range

5–59; 19 females and 16 males), Hispanic/Latino (n=69; median age 70, age range 36–88; 25 females and 44 males), European (n=130; median age 67, age range 40–88; 59 females and 71 males). We adjusted prediction errors by regressing out chronological age from error values before evaluating among-population differences. This was necessary to avoid confounding based on the different age distributions within our cohorts, as prediction accuracy can vary systematically by age for some epigenetic clocks 60. By taking these steps, we ensured that differences in prediction error are not due to sampling design, tissue type, or other technical issues. We identified significant among-population differences in the distribution of age-adjusted prediction errors by ANOVA, followed by a Tukey test to identify significant pairwise differences.

We also assessed the differences in epigenetic age acceleration (EAA) metrics across cohorts (Supplementary Fig. 6). The Horvath residual, Hannum residual, GrimAge, and PhenoAge acceleration metrics are calculated by adjusting the epigenetic age estimated by each predictor for chronological age. Intrinsic epigenetic aging acceleration (EAA) measures the component of EAA that is not influenced by changes in white blood cell count with age (i.e., it is the residual of the Horvath estimate after regressing out both chronological age and DNA methylation-based estimates of blood cell proportions). Extrinsic EAA instead captures both this intrinsic component and age-related changes in white blood cell composition by using the residuals of an enhanced version of the Hannum-based age estimate after regressing out chronological age, but not estimates of blood cell proportions⁷⁸. Positive values of these measures indicate that an individual's predicted age is higher than their actual chronological age. The DNA methylation-based telomere length acceleration estimate is generated by regressing out chronological age from DNA methylation-based estimates of telomere length⁶⁹. Positive values indicate that an individual is estimated to have longer than expected telomeres for their age¹¹⁷. Telomeres tend to get shorter with age and in association with increased risk of age-related diseases118,119

Constructing chronological age predictors

We developed chronological age prediction models using elastic net regression. We selected predictors using the cy.glmnet function in R, employing leave-one-out cross-validation on the training dataset. We conducted 100 different splits of our dataset into training and test sets to construct the heritable and non-heritable prediction models. Each training dataset was created from randomly sampling 70% of the ‡Khomani San and Himba samples and 63% of the Baka samples. For the trios contained in the Baka dataset, children were never included with their parent(s) for training. We trained our models on only the 329,821 CpG sites that were common across all three African cohorts, as well as the 3 saliva-derived validation datasets (European/Hispanic Latino GSE78874 from the established clocks analyses, African-American GSE61653, and Japanese GSE214901) to avoid CpG missingness during validation. The African-American dataset contains 106 females and 22 males, with an age range of 20-74 and a median age of 41.5. The Japanese dataset contains 9 females and 10 males, with an age range of 13-73 and a median age of 61. The heritable models were built by training on 116,132 possible predictor CpGs found to be significantly heritable (p < 0.05) or influenced by meQTL in our baseline scans of any of the three African cohorts. Our non-heritable models were built by training on 213,689 possible predictor CpGs not found to be significantly heritable and not influenced by meQTL in our baseline scans. We conducted a grid search to optimize the alpha parameter for the elastic net regression model. Alpha values ranged from 0 to 1 in increments of 0.05. For each alpha, we used leave-one-out cross-validation on the training data to construct the model and selected the lambda value that minimized the mean squared error (MSE). The best-performing model was then identified based on the alpha value that resulted in the lowest MSE on the held-out test dataset. We used transformed chronological ages following Horvath's method¹² to account for the logarithmic relationship observed at many sites between methylation and age in children and young adults. We then applied each of our 100 heritable and 100 non-heritable epigenetic age prediction models to the validation cohorts of European, Hispanic/Latino, African-American, and Japanese ancestry after first normalizing these data using the wateRmelon¹⁰⁸ package's BMIO function.

Epigenetic aging score (EAS) models

We constructed an EAS for each African population by using the baseline meQTL results to identify SNPs that have a strong influence on DNA methylation levels at a nearby CpG site, retaining only the most significant SNP per CpG site. We intersected this list with each population's meQTL-regressed EWAS results to identify CpG sites that are both influenced by *cis*meQTL and age-associated, using a relaxed significance threshold of 10^{-3} for the latter. We extracted the effect of each SNP allele on CpG methylation and CpG methylation on age to construct the EAS, which is effectively a polygenic score representing the total burden of epigenetic age-increasing genetic variants on an individual's genome, *i* (Eq. 7, Supplementary Fig. 15). The effect of each SNP *j* on age is given by its effect on DNA methylation at the corresponding CpG site, weighted by the effect of DNA methylation level at that CpG site on age. This weighting ensures that the direction of the SNP-on-age effect is consistent across loci, which are then summed to yield an EAS value.

$$EAS \ value_i = \sum_{j}^{N} dosage_{i,j} \times \beta_{j \ on \ CpG \ methylation} \times \beta_{CpG \ methylation \ on \ age} \quad (7)$$

Statistics and Reproducibility

Differences among groups in prediction accuracy were tested via ANOVA with a Tukey adjustment. Differences in prediction accuracy between heritable and non-heritable predictors were tested via a two-sided T-test. Correlations were assessed by calculating Pearson's correlation coefficient using R's cor.test() function using default parameters. Sample sizes for EWAS and meQTL analyses were: Himba (n=51), ‡Khomani San (n=52), and Baka (n=35). Sample sizes for age prediction analyses were limited to those computationally predicted to be from saliva or blood tissue: Himba (n=49), ‡Khomani San (n=46), Baka (n=35), Hispanic/Latino (n=69), and European (n=130). Sample sizes for the age predictor transferability analyses were the Himba (n=49), ‡Khomani San (n=46), Baka (n=35), Hispanic/Latino (n=69), and European (n=130) predicted to be derived from saliva or blood tissues, as well as the African-American (n=64), and Japanese (n=19) saliva-derived samples.

Ethics and Inclusion

Himba community leaders were actively involved in discussions regarding what genetic data could be used for, who would have access to it, and whether there was a for-profit element involved (there was not). Individual informed consent, and for minors, parental assent, was obtained orally from all participants, as most adults in the population were not literate. A record of the Himba oral consent included the participant's name and a local witness (our translator) who was literate and signed for each participant. Oral consent was approved by UCLA and Stony Brook. Permission to work in the community was obtained from Chief Basekama Ngombe. Care was taken to protect participants' privacy, for example, via a double-blind procedure for DNA collection ¹²⁰. These data were collected as part of the longitudinal Kunene Rural Health and Demography Project, which has been working in the community since 2010. The ≠Khomani San samples were collected in 2011, 2012, and 2015 with written informed consent, and the ≠Khomani San participant ages were verified ethnographically on a case-by-case basis. The ≠Khomani San community was sampled non-randomly using an opportunistic sampling strategy. Prior to recruitment, several meetings were held with the local community leaders and town hall meetings open to the whole community. A community member was assigned to the research team as a guide. The research team walked house to house. inviting people to participate. Various documents, such as birth certificates, wedding certificates, school records, and other forms of identification (e.g., apartheid government identification documents), were crossreferenced to identify any inconsistencies. Local major events, such as the creation of the Kalahari National Park in 1931, were also used to verify participants' age. As the Baka communities from Cameroon are illiterate, obtaining written informed consent would have been perceived as an abuse of trust and was therefore avoided. Instead, verbal informed consent was obtained from all adult volunteers and from both parents of any volunteers under the age of 18. Before obtaining consent, the objectives of the study and the sampling protocol were clearly explained to all participants by the social anthropologist Dr Peguy Ndonko (Bamenda University, Cameroon) and the physician and anthropologist, Pr. Alain Froment (Institut de la Recherche et du Développement, France), who had provided medical care to the Baka communities for more than ten years at the time of sampling in 2011 and had built a longterm relationship of trust with them.

Ethical approval

Informed consent was obtained for the collection and analysis of all samples. Ethical approval for the collection of the Himba samples was granted by the University of California, Los Angeles (IRB-10-000238), the State University of New York, Stony Brook (IRB-636415-12), and was approved by the Namibian Ministry of Home Affairs and the University of Namibia Office of Academic Affairs and Research. Chief Basekama Ngombe provided permission to work in the Himba community and local approval of the study. Ethical approval for the collection of DNA samples from the ≠Khomani San was obtained from the Human Research Ethics Committee of Stellenbosch University (N11/07/210), South Africa, and Stanford University (protocol 13829). Ethical approval for the collection of the Baka samples was obtained from the institutional review boards of Institut Pasteur, Paris, France (RBM 2008-06 and 2011-54/IRB/3). All ethical regulations relevant to human research participants were followed.

Reporting summary

Further information on research design is available in the Nature Portfolio Reporting Summary linked to this article.

Data availability

The data from the Baka and ≠Khomani San used in this article have been previously submitted to the European Genome-Phenome Archive (EGA) (www.ebi.ac.uk/ega/home) and GEO. The SNP and methylation array data for the Baka can be found under the EGA accession numbers EGAS00001001066 and EGAS00001002226. The SNP and methylation array data for the ≠Khomani San can be found under the GEO superseries GSE99091. SNP array and methylation array data for the Himba are available via dbGaP, accession phs001995.v3.p1. The European and Hispanic/Latino methylation array dataset can be found under the GEO superseries GSE78874³⁴. The African-American methylation array dataset can be found under the GEO superseries GSE61653⁷⁷. The Japanese methylation array dataset can be found under the GEO superseries GSE214901⁷⁶. The 1000 Genomes Phase 3⁷⁵ data can be accessed via http:// ftp.1000genomes.ebi.ac.uk/vol1/ftp/phase3/. The source data used to create the main text figures are available at https://doi.org/10.5281/zenodo. 15368482¹²¹.

Code availability

Code used to create the main text figures is available at https://doi.org/10. 5281/zenodo.15368482¹²¹ and also available at https://github.com/gillianmeeks/CommsBio_2025_Meeks_etal.

Received: 30 August 2024; Accepted: 15 September 2025; Published online: 05 November 2025

References

- Johansson, A., Enroth, S. & Gyllensten, U. Continuous aging of the human DNA methylome throughout the human lifespan. *PLoS ONE* 8. e67378 (2013).
- Jones, M. J., Goodman, S. J. & Kobor, M. S. DNA methylation and healthy human aging. *Aging Cell* 14, 924–932 (2015).
- Heyn, H. et al. Distinct DNA methylomes of newborns and centenarians. Proc. Natl. Acad. Sci. USA 109, 10522–10527 (2012).
- Weidner, C. I. et al. Aging of blood can be tracked by DNA methylation changes at just three CpG sites. *Genome Biol.* 15, 1–12 (2014).
- Freire-Aradas, A. et al. A common epigenetic clock from childhood to old age. Forensic Sci. Int. Genet. 60, 102743 (2022).
- Vidaki, A. et al. DNA methylation-based forensic age prediction using artificial neural networks and next generation sequencing. Forensic Sci. Int. Genet. 28, 225–236 (2017).
- Eipel, M. et al. Epigenetic age predictions based on buccal swabs are more precise in combination with cell type-specific DNA methylation signatures. *Aging* 8, 1034–1048 (2016).
- Zbieć-Piekarska, R. et al. Development of a forensically useful age prediction method based on DNA methylation analysis. *Forensic Sci. Int. Genet.* 17, 173–179 (2015).
- Cho, S. et al. Independent validation of DNA-based approaches for age prediction in blood. *Forensic Sci. Int. Genet.* 29, 250–256 (2017).
- Jung, S.-E. et al. DNA methylation of the ELOVL2, FHL2, KLF14, C1orf132/MIR29B2C, and TRIM59 genes for age prediction from blood, saliva, and buccal swab samples. Forensic Sci. Int. Genet. 38, 1–8 (2019).
- Dias, H. C. et al. DNA methylation age estimation in blood samples of living and deceased individuals using a multiplex SNaPshot assay. Forensic Sci. Int. 311, 110267 (2020).
- 12. Horvath, S. DNA methylation age of human tissues and cell types. *Genome Biol.* **14**, R115 (2013).
- Hannum, G. et al. Genome-wide methylation profiles reveal quantitative views of human aging rates. *Mol. Cell* 49, 359–367 (2013).
- Jylhävä, J., Pedersen, N. L. & Hägg, S. Biological age predictors. *EBioMedicine* 21, 29–36 (2017).
- 15. Perna, L. et al. Epigenetic age acceleration predicts cancer, cardiovascular, and all-cause mortality in a German case cohort. *Clin. Epigenetics* **8**, 64 (2016).
- Horvath, S. et al. Huntington's disease accelerates epigenetic aging of human brain and disrupts DNA methylation levels. *Aging* 8, 1485–1512 (2016).
- Dugué, P.-A. et al. DNA methylation-based biological aging and cancer risk and survival: pooled analysis of seven prospective studies. *Int. J. Cancer* 142, 1611–1619 (2018).
- 18. Degerman, S. et al. Maintained memory in aging is associated with young epigenetic age. *Neurobiol. Aging* **55**, 167–171 (2017).
- Levine, M. E. et al. An epigenetic biomarker of aging for lifespan and healthspan. Aging 10, 573–591 (2018).
- Lu, A. T. et al. DNA methylation GrimAge strongly predicts lifespan and healthspan. Aging 11, 303 (2019).
- Lu, A. T. et al. DNA methylation GrimAge version 2. Aging 14, 9484–9549 (2022).
- 22. McGreevy, K. M. et al. DNAmFitAge: biological age indicator incorporating physical fitness. *Aging* **15**, 3904–3938 (2023).
- Oblak, L., van der Zaag, J., Higgins-Chen, A. T., Levine, M. E. & Boks, M. P. A systematic review of biological, social and environmental factors associated with epigenetic clock acceleration. *Ageing Res. Rev.* 69, 101348 (2021).
- Gillman, A. S., Pérez-Stable, E. J. & Das, R. Advancing health disparities science through social epigenomics research. *JAMA Netw. Open* 7, e2428992 (2024).

- Chiu, D. T., Hamlat, E. J., Zhang, J., Epel, E. S. & Laraia, B. A.
 Essential nutrients, added sugar intake, and epigenetic age in midlife
 Black and White women: NIMHD social epigenomics program.
 JAMA Netw. Open 7, e2422749 (2024).
- Daredia, S. et al. Prenatal maternal occupation and child epigenetic age acceleration in an agricultural region: NIMHD social epigenomics program. *JAMA Netw. Open* 7, e2421824 (2024).
- Smith, A. K. et al. Epigenetic age acceleration and disparities in posttraumatic stress in women in Southeast Louisiana: NIMHD social epigenomics program. *JAMA Netw. Open* 7, e2421884 (2024).
- Shen, B. et al. Association of race and poverty status with DNA methylation–based age. *JAMA Netw. Open* 6, e236340–e236340 (2023).
- Maunakea, A. K. et al. Socioeconomic status, lifestyle, and DNA methylation age among racially and ethnically diverse adults: NIMHD social epigenomics program. *JAMA Netw. Open* 7, e2421889–e2421889 (2024).
- Krieger, N. et al. Epigenetic aging and racialized, economic, and environmental injustice: NIMHD social epigenomics program. *JAMA Netw. Open* 7, e2421832–e2421832 (2024).
- Harris, K. M. et al. Sociodemographic and lifestyle factors and epigenetic aging in US young adults: NIMHD social epigenomics program. *JAMA Netw. Open* 7, e2427889 (2024).
- Crimmins, E. M., Thyagarajan, B., Levine, M. E., Weir, D. R. & Faul, J. Associations of age, sex, race/ethnicity, and education with 13 epigenetic clocks in a nationally representative U.S. sample: the health and retirement study. *J. Gerontol. A Biol. Sci. Med. Sci.* 76, 1117–1123 (2021).
- Liu, Z. et al. The role of epigenetic aging in education and racial/ ethnic mortality disparities among older U.S. women. Psychoneuroendocrinology 104, 18–24 (2019).
- Horvath, S. et al. An epigenetic clock analysis of race/ethnicity, sex, and coronary heart disease. Genome Biol. 17, 171 (2016).
- Levine, M. E., Lu, A. T., Bennett, D. A. & Horvath, S. Epigenetic age of the pre-frontal cortex is associated with neuritic plaques, amyloid load, and Alzheimer's disease related cognitive functioning. *Aging* 7, 1198–1211 (2015).
- Cruz-González, S. et al. Methylation Clocks Do Not Predict Age or Alzheimer's Disease Risk Across Genetically Admixed Individuals. eLife 14, RP105343 (2025).
- Cronjé, H. T. et al. Comparison of DNA methylation clocks in Black South African men. *Epigenomics* 13, 437–449 (2021).
- Chilunga, F. P. et al. Epigenetic age acceleration in the emerging burden of cardiometabolic diseases among migrant and nonmigrant African populations: the population based cross-sectional RODAM study. *Lancet Healthy Longev.* 2, E327–E339 (2021).
- Sanchez, D. et al. Validity and cardio-metabolic risk profiles of DNA methylation clocks among adults in south-central Côte d'Ivoire. Epigenetics Commun. 2, 1–16 (2022).
- Bell, C. G. et al. DNA methylation aging clocks: challenges and recommendations. *Genome Biol.* 20, 249 (2019).
- Fleckhaus, J., Freire-Aradas, A., Rothschild, M. A. & Schneider, P. M. Impact of genetic ancestry on chronological age prediction using DNA methylation analysis. Forensic Sci. Int. Genet. Suppl. Ser. 6, e399–e400 (2017).
- Thong, Z. et al. Artificial neural network, predictor variables and sensitivity threshold for DNA methylation-based age prediction using blood samples. Sci. Rep. 11, 1–12 (2021).
- Fleckhaus, J., Bugert, P., Al-Rashedi, N. A. M. & Rothschild, M. A. Investigation of the impact of biogeographic ancestry on DNA methylation based age predictions comparing a Middle East and a Central European population. *Forensic Sci. Int. Genet.* 67, 102923 (2023).

- Becker, J. et al. Evidence for differences in DNA methylation between Germans and Japanese. *Int. J. Leg. Med.* 136, 405–413 (2022).
- Martin, A. R. et al. Clinical use of current polygenic risk scores may exacerbate health disparities. *Nat. Genet.* 51, 584–591 (2019).
- Bonder, M. J. et al. Disease variants alter transcription factor levels and methylation of their binding sites. *Nat. Genet.* 49, 131–138 (2017).
- 47. Bergstedt, J. et al. The immune factors driving DNA methylation variation in human blood. *Nat. Commun.* **13**, 5895 (2022).
- Min, J. L. et al. Genomic and phenotypic insights from an atlas of genetic effects on DNA methylation. *Nat. Genet.* 53, 1311–1321 (2021).
- Villicaña, S. & Bell, J. T. Genetic impacts on DNA methylation: research findings and future perspectives. *Genome Biol.* 22, 127 (2021).
- Fraser, H. B., Lam, L. L., Neumann, S. M. & Kobor, M. S. Populationspecificity of human DNA methylation. *Genome Biol.* 13, R8 (2012).
- Heyn, H. et al. DNA methylation contributes to natural human variation. Genome Res. 23, 1363–1372 (2013).
- 52. Rahmani, E. et al. Genome-wide methylation data mirror ancestry information. *Epigenetics Chromatin* **10**, 1 (2017).
- Carja, O. et al. Worldwide patterns of human epigenetic variation.
 Nat. Ecol. Evol. 1, 1577–1583 (2017).
- Galanter, J. M. et al. Differential methylation between ethnic subgroups reflects the effect of genetic ancestry and environmental exposures. *eLife* 6, e20532 (2017).
- Husquin, L. T. et al. Exploring the genetic basis of human population differences in DNA methylation and their causal impact on immune gene regulation. *Genome Biol.* 19, 222 (2018).
- Lu, A. T. et al. GWAS of epigenetic aging rates in blood reveals a critical role for TERT. Nat. Commun. 9, 387 (2018).
- 57. Genetics, N. A reference panel of 64,976 haplotypes for genotype imputation. *Nat. Genet.* **48**, 1279–1283 (2016).
- Horvath, S. et al. Epigenetic clock for skin and blood cells applied to Hutchinson Gilford Progeria Syndrome and ex vivo studies. *Aging* 10, 1758–1775 (2018).
- Zhang, Q. et al. Improved precision of epigenetic clock estimates across tissues and its implication for biological ageing. *Genome Med* 11, 54 (2019).
- El Khoury, L. Y. et al. Systematic underestimation of the epigenetic clock and age acceleration in older subjects. *Genome Biol.* 20, 1–10 (2019).
- McManus, K. F. et al. Population genetic analysis of the DARC locus (Duffy) reveals adaptation from standing variation associated with malaria resistance in humans. *PLoS Genet.* 13, e1006560 (2017).
- 62. Reich, D. et al. Reduced neutrophil count in people of African descent is due to a regulatory variant in the Duffy antigen receptor for chemokines gene. *PLoS Genet.* **5**, e1000360 (2009).
- Merz, L. E. et al. Absolute neutrophil count by Duffy status among healthy Black and African American adults. *Blood Adv.* 7, 317–320 (2023)
- Bagheri, M. et al. White blood cell ranges and frequency of neutropenia by Duffy genotype status. *Blood Adv.* 7, 406–409 (2023).
- 65. Howes, R. E. et al. The global distribution of the Duffy blood group. *Nat. Commun.* **2**, 266 (2011).
- Uren, C. et al. Fine-scale human population structure in Southern Africa reflects ecogeographic boundaries. *Genetics* 204, 303–314 (2016).
- Teschendorff, A. E., Breeze, C. E., Zheng, S. C. & Beck, S. A comparison of reference-based algorithms for correcting cell-type heterogeneity in Epigenome-Wide Association Studies. *BMC Bioinform.* 18, 105 (2017).

- Langie, S. A. S. et al. Salivary DNA methylation profiling: aspects to consider for biomarker identification. *Basic Clin. Pharmacol. Toxicol.* 121, 93–101 (2017).
- 69. Lu, A. T. et al. DNA methylation-based estimator of telomere length. *Aging* **11**, 5895–5923 (2019).
- Gopalan, S. et al. Trends in DNA methylation with age replicate across diverse human populations. *Genetics* 206, 1659–1674 (2017).
- Gusev, A. et al. Integrative approaches for large-scale transcriptome-wide association studies. *Nat. Genet.* 48, 245–252 (2016).
- Purcell, S. et al. PLINK: a tool set for whole-genome association and population-based linkage analyses. *Am. J. Hum. Genet.* 81, 559–575 (2007).
- Wang, G., Sarkar, A., Carbonetto, P. & Stephens, M. A simple new approach to variable selection in regression, with application to genetic fine mapping. J. R. Stat. Soc. Ser. B Stat. Methodol. 82, 1273–1300 (2020).
- Henn, B. M., Botigué, L. R., Bustamante, C. D., Clark, A. G. & Gravel, S. Estimating the mutation load in human genomes. *Nat. Rev. Genet.* 16, 333–343 (2015).
- 1000 Genomes Project Consortium et al. A global reference for human genetic variation. Nature 526, 68–74 (2015).
- Nishitani, S. et al. Cross-tissue correlations of genome-wide DNA methylation in Japanese live human brain and blood, saliva, and buccal epithelial tissues. *Transl. Psychiatry* 13, 72 (2023).
- Smith, A. K. et al. DNA extracted from saliva for methylation studies of psychiatric traits: evidence tissue specificity and relatedness to brain. Am. J. Med. Genet. B Neuropsychiatr. Genet. 168B, 36–44 (2015).
- Chen, B. H. et al. DNA methylation-based measures of biological age: meta-analysis predicting time to death. *Aging* 8, 1844–1865 (2016).
- Marioni, R. E. et al. The epigenetic clock is correlated with physical and cognitive fitness in the Lothian Birth Cohort 1936. *Int. J. Epidemiol.* 44, 1388–1396 (2015).
- Marioni, R. E. et al. DNA methylation age of blood predicts all-cause mortality in later life. *Genome Biol.* 16, 25 (2015).
- Gibson, J. et al. A meta-analysis of genome-wide association studies of epigenetic age acceleration. *PLoS Genet.* 15, e1008104 (2019).
- 82. Maddock, J. et al. DNA methylation age and physical and cognitive aging. *J. Gerontol. A Biol. Sci. Med. Sci.* **75**, 504–511 (2020).
- Hillary, R. F. et al. An epigenetic predictor of death captures multimodal measures of brain health. *Mol. Psychiatry* 26, 3806–3816 (2021).
- McCrory, C. et al. GrimAge outperforms other epigenetic clocks in the prediction of age-related clinical phenotypes and all-cause mortality. J. Gerontol. A Biol. Sci. Med. Sci. 76, 741–749 (2021).
- Ryan, J., Wrigglesworth, J., Loong, J., Fransquet, P. D. & Woods, R. L. A systematic review and meta-analysis of environmental, lifestyle, and health factors associated with DNA methylation age. *J. Gerontol. A Biol. Sci. Med. Sci.* 75, 481–494 (2020).
- Privé, F. et al. Portability of 245 polygenic scores when derived from the UK Biobank and applied to 9 ancestry groups from the same cohort. Am. J. Hum. Genet. 109, 373 (2022).
- Wang, Y., Tsuo, K., Kanai, M., Neale, B. M. & Martin, A. R. Challenges and opportunities for developing more generalizable polygenic risk scores. *Annu Rev. Biomed. Data Sci.* 5, 293–320 (2022).
- Polygenic Risk Score Task Force of the International Common Disease Alliance. Responsible use of polygenic risk scores in the clinic: potential benefits, risks and gaps. *Nat. Med.* 27, 1876–1884 (2021).
- Fagny, M. et al. The epigenomic landscape of African rainforest hunter-gatherers and farmers. *Nat. Commun.* 6, 10047 (2015).

- DNA Methylation Age Calculator. https://dnamage.clockfoundation.org (2024).
- 91. Non, A. L. Social epigenomics: are we at an impasse?. *Epigenomics* **13**, 1747 (2021).
- 92. Ragsdale, A. P. et al. A weakly structured stem for human origins in Africa. *Nature* **617**. 755–763 (2023).
- 93. Zenin, A. et al. Identification of 12 genetic loci associated with human healthspan. *Commun. Biol.* **2**, 1–11 (2019).
- 94. Kim, Y. et al. Higher diet quality relates to decelerated epigenetic aging. *Am. J. Clin. Nutr.* **115**, 163–170 (2022).
- Gindin, Y. et al. DNA methylation and immune cell markers demonstrate evidence of accelerated aging in patients with chronic hepatitis B virus or hepatitis C virus, with or without human immunodeficienct virus coinfection. *Clin. Infect. Dis.* 73, e184–e190 (2021).
- Durso, D. F. et al. Living in endemic area for infectious diseases accelerates epigenetic age. Mech. Ageing Dev. 207, 111713 (2022).
- 97. Palma-Gudiel, H., Fañanás, L., Horvath, S. & Zannas, A. S. Psychosocial stress and epigenetic aging. *Int. Rev. Neurobiol.* **150**, 107–128 (2020).
- Gao, X., Zhang, Y., Breitling, L. P. & Brenner, H. Relationship of tobacco smoking and smoking-related DNA methylation with epigenetic age acceleration. *Oncotarget* 7, 46878–46889 (2016).
- 99. Bollig, M. Risk and risk minimisation among Himba pastoralists in northwestern Namibia. *Nomad. People* **1**, 66–89 (1997).
- Prall, S. & Scelza, B. The dietary impacts of drought in a traditional pastoralist economy. Am. J. Hum. Biol. 35, e23803 (2023).
- 101. Dieckmann, U. The status of food security and nutrition of San Communities in Southern Africa. Preprint at https://www.researchgate.net/profile/Ute-Dieckmann/publication/343628289_The_Status_of_Food_Security_and_Nutrition_of_San_Communities_in_Southern_Africa/links/5f350444299bf13404be866e/The-Status-of-Food-Security-and-Nutrition-of-San-Communities-in-Southern-Africa.pdf (2018).
- Gallois, S. & Henry, A. G. The cost of gathering among the Baka forager-horticulturalists from southeastern Cameroon. *Front. Ecol. Evol.* 9, 768003 (2021).
- Price, M. E. et al. Additional annotation enhances potential for biologically-relevant analysis of the Illumina Infinium HumanMethylation450 BeadChip array. Epigenetics Chromatin 6, 4 (2013).
- Pidsley, R. et al. Critical evaluation of the Illumina MethylationEPIC BeadChip microarray for whole-genome DNA methylation profiling. Genome Biol. 17, 208 (2016).
- Meeks, G. L., Henn, B. M. & Gopalan, S. Genetic differentiation at probe SNPs leads to spurious results in meQTL discovery. Commun. Biol. 6, 1–4 (2023).
- gillianmeeks & Gopalan, S. gillianmeeks/probeSNPffer: probeSNPffer. Zenodo https://doi.org/10.5281/ZENODO. 10067504 (2023).
- Zhi, D. et al. SNPs located at CpG sites modulate genomeepigenome interaction. *Epigenetics* 8, 802–806 (2013).
- Pidsley, R. et al. A data-driven approach to preprocessing Illumina
 450K methylation array data. BMC Genomics 14, 293 (2013).
- Aryee, M. J. et al. Minfi: a flexible and comprehensive Bioconductor package for the analysis of Infinium DNA methylation microarrays. *Bioinformatics* 30, 1363–1369 (2014).
- Delaneau, O., Marchini, J. & Zagury, J.-F. A linear complexity phasing method for thousands of genomes. *Nat. Methods* 9, 179–181 (2011).
- Durbin, R. Efficient haplotype matching and storage using the positional Burrows–Wheeler transform (PBWT). *Bioinformatics* 30, 1266–1272 (2014).
- Kang, H. M. et al. Variance component model to account for sample structure in genome-wide association studies. *Nat. Genet.* 42, 348–354 (2010).

- Lehne, B. et al. A coherent approach for analysis of the Illumina HumanMethylation450 BeadChip improves data quality and performance in epigenome-wide association studies. *Genome Biol.* 16, 37 (2015).
- Li, Z. & Wu, H. TOAST: improving reference-free cell composition estimation by cross-cell type differential analysis. *Genome Biol.* 20, 190 (2019).
- 115. Schwarzer, G. meta: an R package for meta-analysis. *R. N.* **7**, 40–45 (2007).
- Yang, J., Lee, S. H., Goddard, M. E. & Visscher, P. M. GCTA: a tool for genome-wide complex trait analysis. *Am. J. Hum. Genet.* 88, 76–82 (2011).
- Nordfjäll, K., Svenson, U., Norrback, K.-F., Adolfsson, R. & Roos, G. Large-scale parent-child comparison confirms a strong paternal influence on telomere length. Eur. J. Hum. Genet. 18, 385–389 (2010).
- Aviv, A. & Shay, J. W. Reflections on telomere dynamics and ageingrelated diseases in humans. *Philos. Trans. R. Soc. Lond. B Biol. Sci.* 373, 20160436 (2018).
- Needham, B. L. et al. Leukocyte telomere length and mortality in the National Health and Nutrition Examination Survey, 1999-2002. Epidemiology 26, 528–535 (2015).
- Scelza, B. A. et al. The ethics and logistics of field-based genetic paternity studies. Evol. Hum. Sci. 2, 1–36 (2020).
- Meeks, G. & Gopalan, S. Common DNA sequence variation influences epigenetic aging in African populations. Zenodo https:// doi.org/10.5281/ZENODO.15368482 (2025).

Acknowledgements

We would like to thank the Working Group of Indigenous Minorities in Southern Africa and the South African San Institute for their advice regarding community research. We thank the Himba, ≠Khomani San, and Baka communities in which we have sampled; without their support, this study would not have been possible. The authors acknowledge the High Performance Computing Core Facility at the University of California, Davis and the Center for Human Genetics Research Computing at Clemson University for providing computational resources that have contributed to the research results reported in this paper. B.M.H. and G.L.M. were supported by the National Institutes of Health grant R35GM133531. S.G. was supported by the National Institutes of Health Center of Biomedical Research Excellence grant 1P20GM139769 and the National Institute of Justice grant 2016-DN-BX-0011. B.S. was supported by the National Science Foundation grant BCS-1534682. The content is solely the responsibility of the authors and does not necessarily represent the official views of the National Institutes of Health, National Science Foundation, or National Institute of Justice. The funders had no role in the decision to publish or prepare the manuscript. Graphical abstract designed by Melisa Morales from Science Graphic Design.

Author contributions

S.G. and G.L.M. conducted analyses. S.G. and G.L.M. wrote the manuscript with input from all authors. B.S., S.P., E.P., A.F., M.F., and L.Q. contributed data for analyses. H.M.A. conducted preliminary analyses on newly generated data. S.G. and B.M.H. conceived and supervised the study.

Competing interests

The authors declare no competing interests.

Additional information

Supplementary information The online version contains supplementary material available at https://doi.org/10.1038/s42003-025-08893-0.

Correspondence and requests for materials should be addressed to Shyamalika Gopalan.

Peer review information Communications Biology thanks Felix Chilunga and the other anonymous reviewer(s) for their contribution to the peer review of this work. Primary Handling Editor: Aylin Bircan. A peer review file is available.

Reprints and permissions information is available at http://www.nature.com/reprints

Publisher's note Springer Nature remains neutral with regard to jurisdictional claims in published maps and institutional affiliations.

Open Access This article is licensed under a Creative Commons Attribution-NonCommercial-NoDerivatives 4.0 International License, which permits any non-commercial use, sharing, distribution and reproduction in any medium or format, as long as you give appropriate credit to the original author(s) and the source, provide a link to the Creative Commons licence, and indicate if you modified the licensed material. You do not have permission under this licence to share adapted material derived from this article or parts of it. The images or other third party material in this article are included in the article's Creative Commons licence, unless indicated otherwise in a credit line to the material. If material is not included in the article's Creative Commons licence and your intended use is not permitted by statutory regulation or exceeds the permitted use, you will need to obtain permission directly from the copyright holder. To view a copy of this licence, visit https://creativecommons.org/licenses/by-nc-nd/4.0/.

© The Author(s) 2025